Quaternary tectonics and present stress tensor of the inverted northern Falcón Basin, northwestern Venezuela

Franck A. Audemard M.

FUNVISIS, Apartado postal 76880, Caracas 1070-A, Venezuela

Abstract

The Tertiary Falcón Basin in northwestern Venezuela has a privileged position in the geodynamic puzzle of northwestern South America, occurring in a region where several major plates (Caribbean, South America and Nazca) and minor lithospheric blocks (Maracaibo, Bonaire and Western Colombia) are interacting. A combination of good exposures due to aridity and a near-continuous sedimentary record in a now inverted basin helps to unravel the Neogene and Quaternary geodynamic evolution of this region. A neotectonic and microtectonic investigation of the Plio-Quaternary sedimentary rocks of the northern Falcón Basin reveals that this region is subject to a compressive to transpressive regime at present. This regime is characterized by a NNW–SSE oriented maximum horizontal stress, and a ENE–WSW trending intermediate (or minimum) horizontal stress, as is confirmed by focal mechanism solutions. This stress field is in agreement both with the NNE-directed extrusion of the Maracaibo and Bonaire blocks in Western Venezuela, where the Falcón Basin is located, and present-day transpression along the Caribbean-South America plate boundary zone. © 2001 Elsevier Science Ltd. All rights reserved.

1. Introduction

The geology of northern and western Venezuela records the geodynamic jostling between the South America, Nazca and Caribbean plates. In fact, northern Venezuela essentially lies in the interaction zone between the South America and Caribbean plates, whereas western Venezuela shows a more complex geodynamic setting. Consequently, the Tertiary Falcón Basin in northwestern Venezuela should shed light on the Tertiary and Quaternary evolution of this complex corner of the South American continent, where three major plates and several smaller crustal blocks are interacting (Audemard, 1993; 1998b). Furthermore, the value of this basin is enhanced by the fact that its sedimentary record is well preserved by the arid climate and has been almost perfectly continuous since the Upper Eocene.

2. Geodynamic setting

A wide consensus establishes that the Caribbean plate moves eastward relative to South America (Bell, 1972; Malfait and Dinkelman, 1972; Jordan, 1975; Pindell and Dewey, 1982; Sykes et al., 1982; Wadge and Burke, 1983; Freymueller et al., 1993 among others). However,

this active plate boundary is not of the simple right-lateral type (Soulas, 1986; Beltrán, 1994). Instead, it constitutes a >100-km-wide active transpressional zone (Audemard, 1993; Singer and Audemard, 1997; Audemard, 1998b) with significant associated topographic relief (the Coast and Interior ranges along the northern coast). This diffuse transpressional boundary zone extends southwestard into the Mérida Andes, where strain is partitioned between the right-lateral strike-slip Boconó fault running along the axis of the chain and the thrust faults bounding the chain on both foothills (Fig. 1 inset). This configuration, both in the Andes and in the Interior Range, was described by Rod (1956) and others long before the concept of "partitioning" was put forward. Within this transpressional boundary zone, a large portion of the right-lateral motion seems to take place along the major right-lateral strike-slip Boconó-San Sebastián-El Pilar-Los Bajos fault system (Molnar and Sykes, 1969; Minster and Jordan, 1978; Pérez and Aggarwal, 1981; Schubert, 1984; Stephan, 1982; 1985; Soulas, 1986; Beltrán and Giraldo, 1989; Singer and Audemard, 1997).

Conversely, the plate boundary in western Venezuela, where the now-inverted Falcón Basin lies, is up to 600 km wide and comprises a set of discrete tectonic blocks (e.g. the Maracaibo and Bonaire blocks), independently moving among the surrounding larger plates (Caribbean, South America and Nazca). For instance, the discrete Maracaibo block is bounded by the left-lateral strike-slip Santa

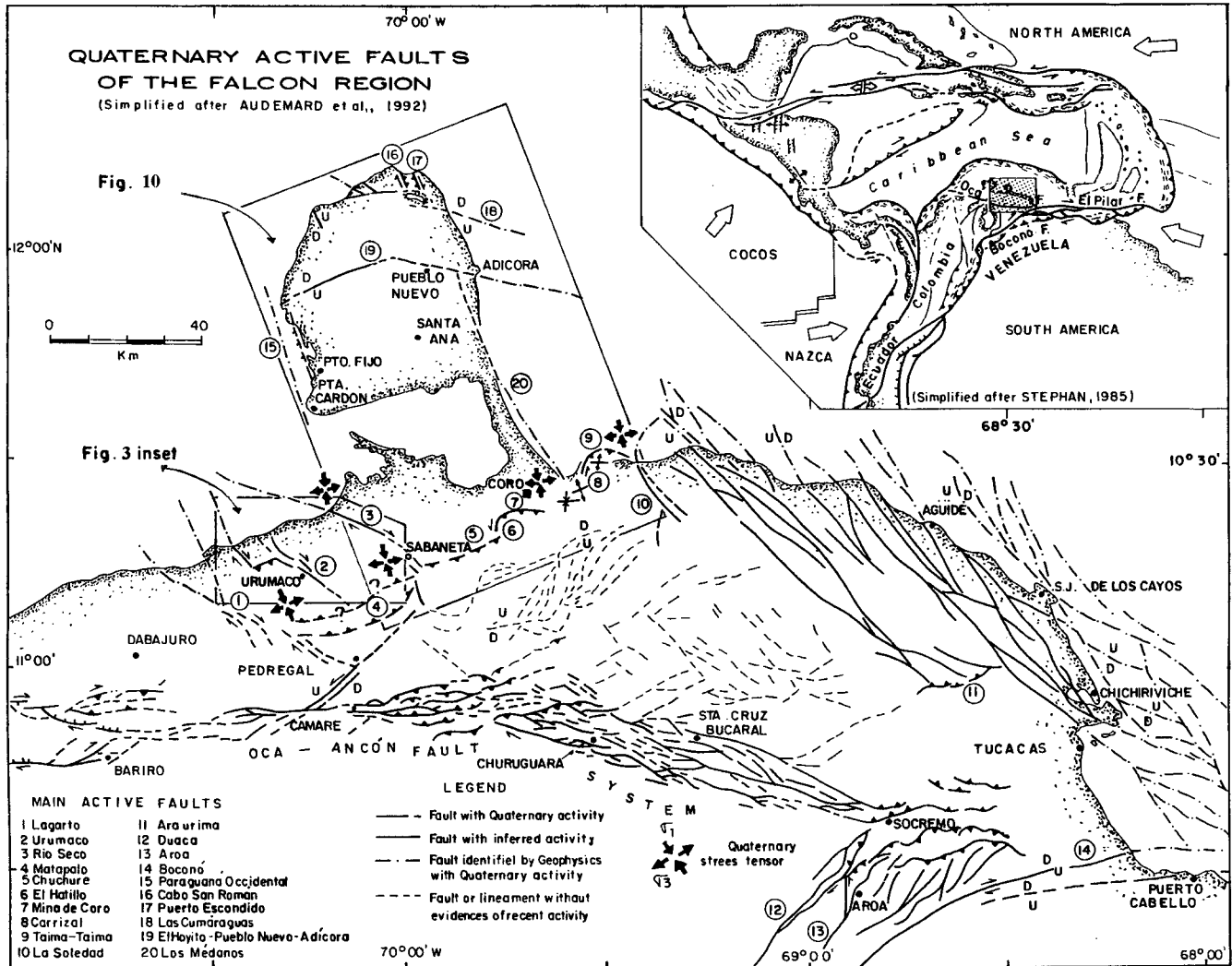*E-mail address:* faudem@funvisis.internet.ve (F.A. Audemard).

Fig. 1. Quaternary active faults of the Falcón region in northwestern Venezuela (simplified after Audemard et al., 1992). Small inset at upper right corner shows relative location at plate tectonics scale. Relative location of Fig. 3 inset and Fig. 10 are also shown.

Marta–Bucaramanga fault in Colombia and Boconó fault in Venezuela, and it is separated on the north from the Bonaire block by the right-lateral strike-slip Oca–Ancón fault (Fig. 1 inset). In addition, both Maracaibo and Bonaire blocks are being extruded roughly northward and are overriding the Caribbean plate north of the Leeward Antilles islands, where a young south-dipping, flat subduction zone has been forming, mainly in the last 5 Ma (Audemard, 1993). Extrusion of these blocks is related to the collision of the Panamá Arc against the Pacific edge of northern South America and its subsequent suturing (Audemard, 1993; 1998b).

Therefore, the Caribbean–South America and Caribbean–Bonaire–Maracaibo boundaries have been mainly affected by transpression (compressive-transcurrent regime) during the Tertiary. This is consistent with early plate motion vectors (WNW–ESE oriented) proposed by Jordan (1975) and Minster and Jordan (1978) and later confirmed by recent GPS geodetic measurements (Freymueller et al., 1993).

Besides, this present Caribbean–South American geodynamic configuration results from a transpressive evolution that has occurred throughout the Tertiary and Quaternary, initiated as an oblique type-B subduction (NW-dipping, South American-attached oceanic lithosphere sinking under Caribbean plate island arc), which later evolved into a long-lasting, east-younging oblique-collision (SSE-vergent Caribbean-affinity nappes overriding South America passive margin) and in turn has shifted to transpression when and where collision became unsustainable (Audemard, 1993; 1998b).

3. Geologic setting

The Tertiary Falcón Basin outcrops for some 36 000 km^2, comprising several states of northwestern Venezuela: the whole of Falcón and parts of Zulia, Lara and Yaracuy. Compilation and integration of regional lithostratigraphic
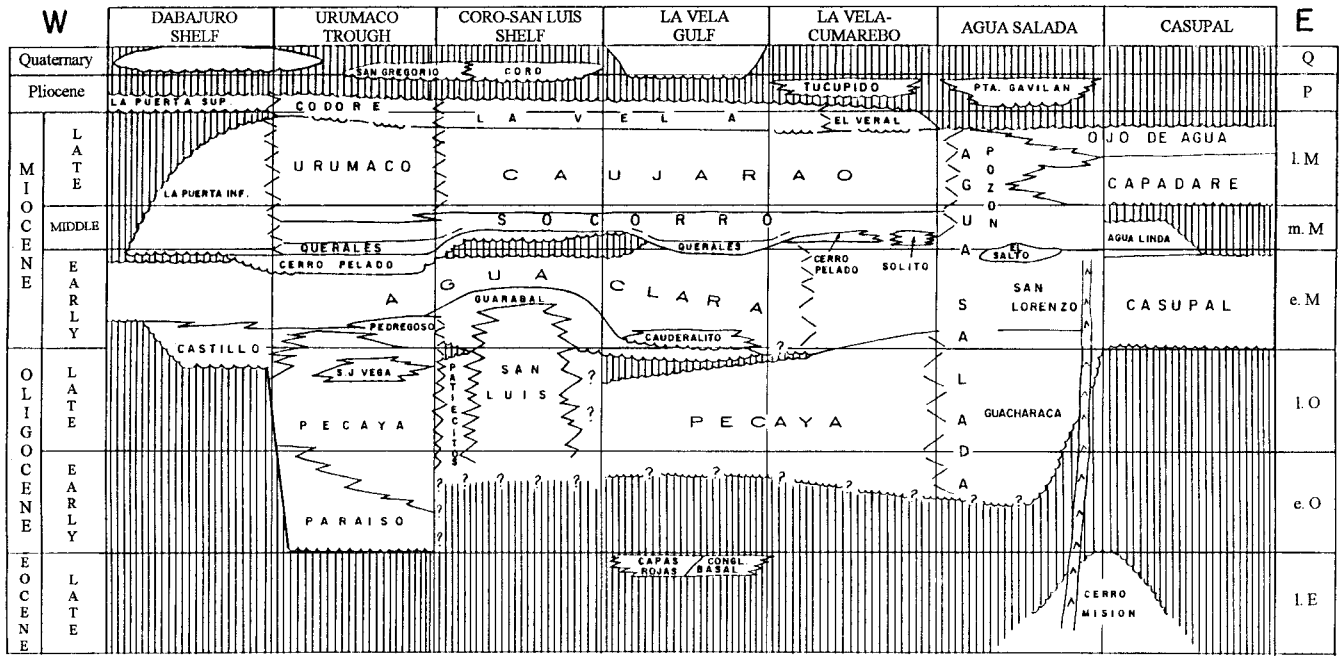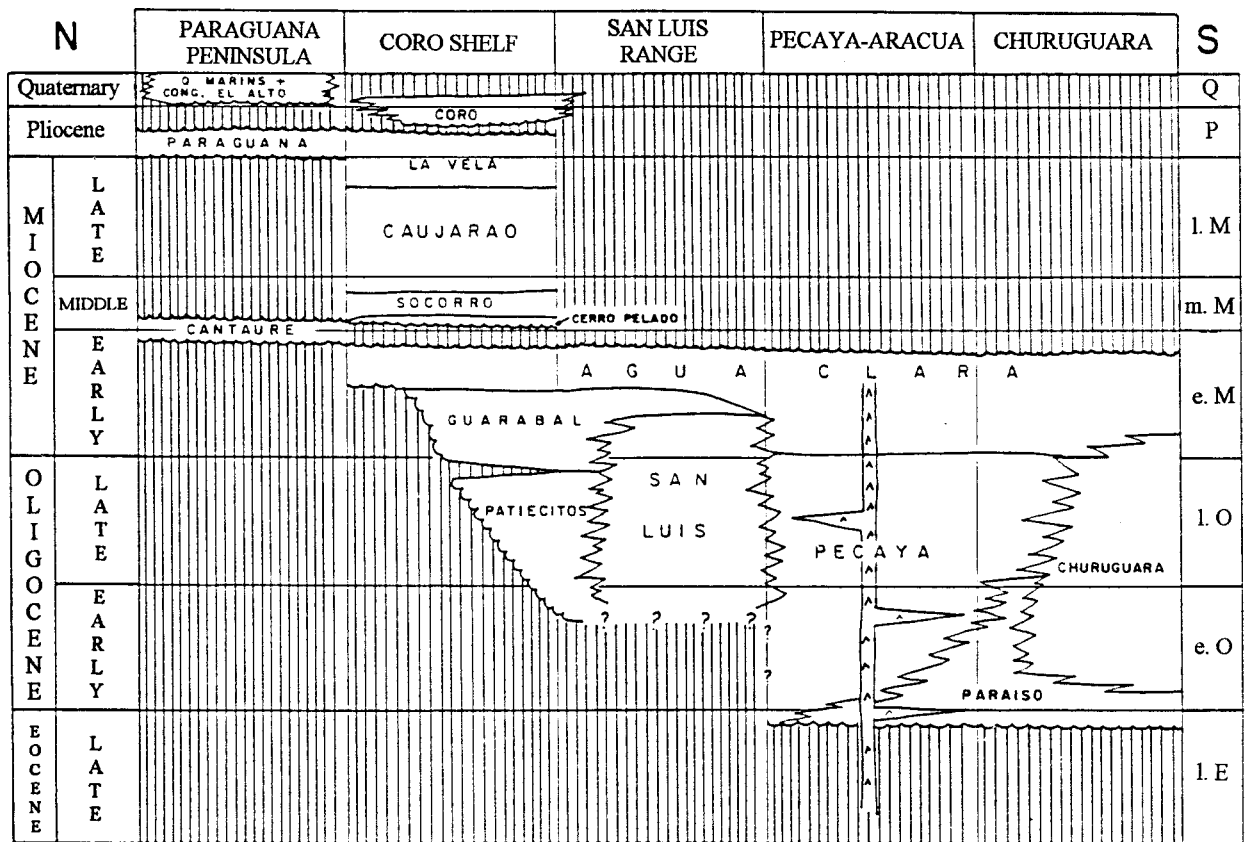
Fig. 2. Stratigraphic correlation charts across the Falcón Basin (Audemard (1993)): (a) west–east oriented correlation, showing the local development of three unconformities but with regional significance; (b) stratigraphic correlation chart in a north-south direction, showing how sedimentation from the Middle Miocene unconformity has been restricted to the northern flank of the Falcón Anticlinorium.

charts (Fig. 2a and b) have allowed Audemard (1993) to establish six key points. First, the sedimentary record of the Falcón Basin is almost continuous since the Upper

Eocene, with the exception of three angular and/or erosional unconformities which although of some regional extent are not always widespread throughout the entire basin (e.g.

absent in the Urumaco Trough and in its eastern marine side). Second, the marine Oligo-Miocene Falcón Basin used to be the western deadend of the still active Bonaire Basin, presently offshore of the Venezuelan Coast Range, until it was intensively folded and tectonically inverted by NW–SE compression in Middle and Upper Miocene times to form an ENE–WSW-trending anticlinorium. Third, sedimentation in this region has been restricted exclusively to the north flank of the Falcón Anticlinorium, where sedimentary sequences since the first inversion phase have progressively become less marine and more continental. Fourth, basin inversion has been active until at least the Lower Pleistocene based on the following observations: (1) the upright form of Pliocene shallow marine deposits (La Vela Formation) along the north limb of La Vela Anticline; (2) the steep (65° to the north) dip of Plio-Pleistocene fan-conglomerates (Coro Formation); and (3) the existence of two younger (Pliocene and Pleistocene) unconformities. Moreover, ongoing tectonic inversion is suggested by emergent Quaternary marine features (e.g. beachrocks, staircase-like flights of marine terraces) along the northern coast of this region (Audemard, 1996a, b; Audemard et al., 1997). Fifth, wrenching activation between the Bonaire and Maracaibo blocks along the Oca-Ancón fault system only started at around 17–15 Ma, coeval with onset of basin inversion and end of axial volcanism. Finally, the last tectonic phase is essentially Upper Pliocene to Quaternary in age, thus restricting neotectonic studies to geologic units of that age. It is this neotectonic phase that this paper seeks to elucidate, principally by using the analysis of fault slip data derived from kinematic indicators on fault surfaces (collectively termed "microtectonic" data in this paper) to reveal the recent stress field history of the Falcón Basin.

4. Neotectonic-microtectonic studies

Taking into account the good chronology of the Neogene evolution of the Falcón Basin derived from the lithostratigraphic revaluation of its sedimentary fill (Audemard, 1993, 1998a), extensive field investigations were undertaken in the northern portion of the State of Falcón to identify brittle and ductile deformation structures affecting the Pliocene and Pleistocene formations. The tectonic inversion coupled with the climatic aridity combine to make excellent exposures, particularly in the Urumaco Trough (southwest of Coro) and the Paraguaná Peninsula, that are ideal for stress tensor and neotectonic analyses.

There were two phases to the study. First, a thorough analysis of air photos (1:8000, 1:25 000 and 1:50 000 scale) was undertaken to identify landforms diagnostic of Quaternary faulting (cf. Vedder and Wallace, 1970; Wesson et al., 1975; Slemmons, 1977) and thrust-related folding (see Audemard, 1999). Second, field verifications of the identified geomorphic evidence of faulting or folding were

carried out. The fieldwork involved three main procedures: (1) detailed logging of the outcrop to record mesoscopic geometric and/or chronologic relationships among tectonic and sedimentary structures; (2) determination of fault slip from kinematic indicators on fault surface (steps, strilolites, Riedel shears, recrystallizations, stylolitic peaks (slickolites), tool marks and, occasionally, gypsum fiber growth) akin to those described by Tjia (1971); Mattauer (1973); Proust et al. (1977); Petit et al. (1983); Hancock and Barka (1987); Angelier (1994); and (3) measurement of the throws and offsets of surface faults, mainly using cross-cutting relationships between tectonic structures and planar sedimentary features.

Stress tensors were subsequently derived from fault populations using the automated inverse method developed by Etchecopar et al. (1981). This method, as many others, is based on the Bott's principle (Bott, 1959), which determines the stress tensor by minimizing the deviation between the shear stress and the observed slip on fault surfaces. Consequently, this tensor calculation depends strongly on determining correctly the sense of slip on each fault of a set; this is obtained from the demonstrating that different kinematic indicators are persistent and consistent on a fault plane. While a few faults were suitable for paleoseismic assessments (e.g. Oca and Ancón (Audemard, 1996c) and Urumaco (Audemard et al., 1999a)), several had a poor geomorphic expression and could only be mapped using conventional surface geology studies. The results of the air photo and field mapping are shown in Fig. 1.

The pattern and kinematics of faulting and folding (Fig. 1) confirms that the northern Falcón Basin is undergoing a stress tensor characterized by a NNW–SSE to north–south maximum horizontal stress and an ENE–WSW minimum (or intermediate) horizontal stress (Audemard, 1993; Audemard, 1997). This is analogous to the simple shear model associated with strike-slip faulting proposed by Wilcox et al. (1973). In addition, Fig. 1 suggests that active tectonic structures in this region can be distinguished into five families on the basis of their orientation and kinematics (Audemard, 1993; Audemard and Singer, 1996; Audemard, 1997). These five families are: (1) east–west-striking right-lateral faults (Oca-Ancón Fault System, Adícora Fault); (2) NW–SE-striking right-lateral faults, synthetic to the east–west-striking faults (Urumaco, Río Seco, Lagarto and La Soledad faults); (3) NNW–SSE striking normal faults (Western Paraguaná, Cabo San Román, Puerto Escondido and Los Médanos faults); (4) north–south-to-NNE–SSW-striking left-lateral faults, antithetic to the east–west-striking faults (Carrizal, El Hatillo and other minor faults); and (5) ENE–WSW-striking reverse faults, parallel to folding axis (Araurima, Taima–Taima, Chuchure and Matapalo faults).

The objective of this paper is to verify this regional assessment of the tectonic stress field with detailed microtectonic analyses from principal fault zones in the northern Falcón Basin. In the following section, the results of
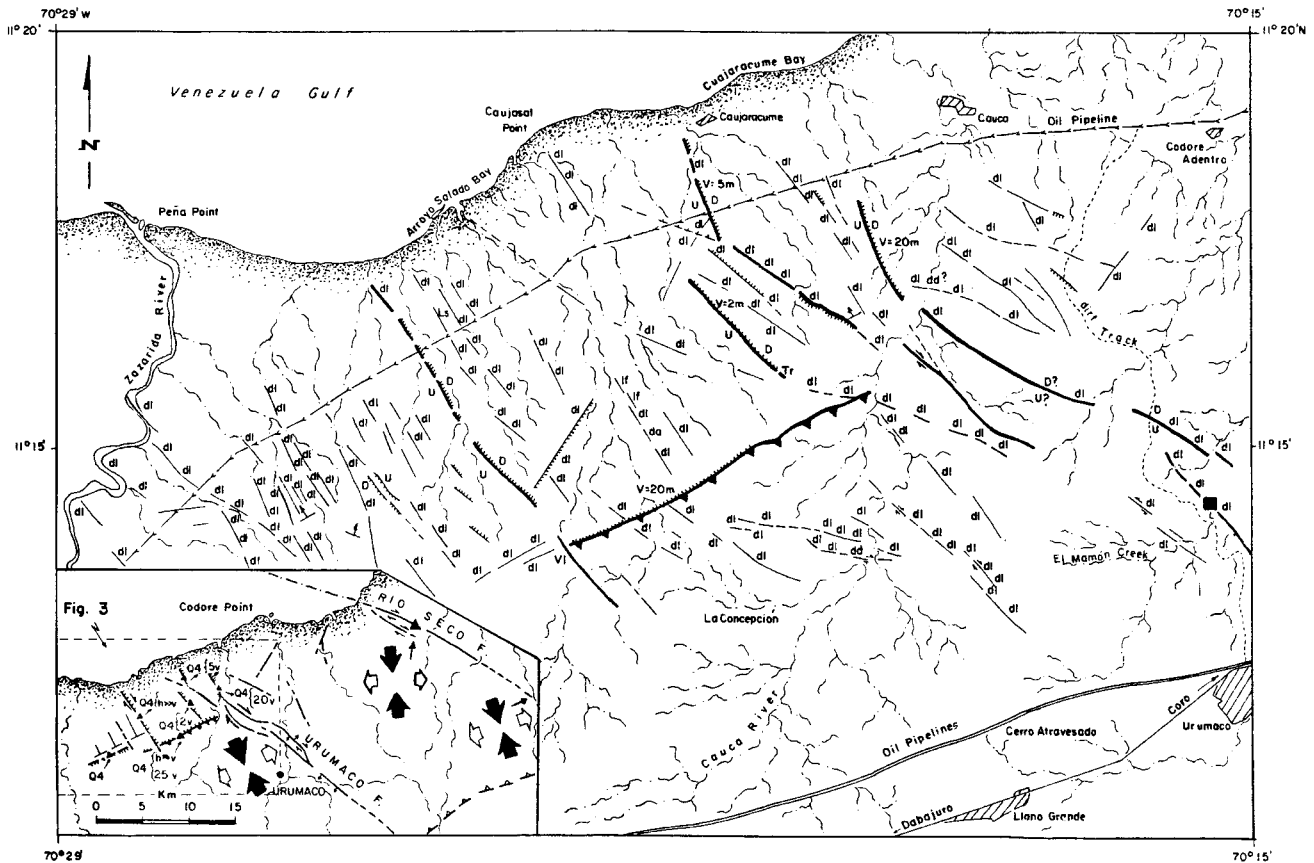
Fig. 3. Geomorphic evidence of Quaternary tectonic activity along the Urumaco Fault, between the Zazárida and Urumaco rivers, southwest of Coro (Audemard, 1993). Small inset shows relative location of this figure, as well as Quaternary stress tensors calculated by Audemard (1993; 1997) in the Urumaco Trough. Legend: dd, offset drainage; dl, linear drainage; lf, linear ridge; ls, line spring; tr, trench; U/D, up/down; 10 v, 10 m of vertical throw; h ≈ v, similar horizontal and vertical offsets; Q_4 = Lower Pleistocene, relative age of deformed geologic marker (Q_0 is younger than Q_1 and consecutively); bold lines indicate active fault traces; barbed lines represent fault scarps. Legend is also valid for other figures, such as Fig. 10.

detailed mapping and stress-tensor determinations are presented for three principal onshore faults: the Urumaco, Río Seco and Taima–Taima faults. In addition, key neotectonic aspects of the Paraguaná Peninsula, which further constrain the timing of the present stress tensor, are briefly discussed. The entire microtectonic data set is available from the author, or can be accessed from Audemard (1993).

5. The Urumaco Fault

5.1. Active trace

The Urumaco Fault extends in NW–SE direction for over 30 km in length, affecting Upper Miocene age and younger sedimentary rocks of the Urumaco Trough, a sub-basin of the Falcón Basin, located southwest of Coro. The Quaternary trace of the fault is not simple, displaying two distinct 10-km-apart segments, linked by an ENE–WSW reverse fault (Fig. 3 and inset), arranged as a restraining stepover (Audemard, 1993). A detailed description of the neotectonic aspects of the Urumaco fault is given by Audemard et al. (1999a), but its right-lateral sense of slip has been established

by geomorphic evidence (i.e. right-laterally offset drainages; Fig. 3), by offset Neogene strata, and, as discussed below, by consistent and persistent fault-plane kinematic indicators observed at three river cuts.

5.2. Microtectonics

The sense of slip, and associated stress tensor, characterising the most recent phase of activity along the Urumaco Fault, has been assessed along its eastern segment — the longest onshore strand — at three river cuts located 3 km north of the Urumaco village. Two sections occur on an ephemeral tributary (Mamón Creek) of the Urumaco River (black square on east edge of Fig. 3) and one section occurs on the Urumaco River itself. In all three sections, fault planes of the main segment cut sediments of the Upper Miocene Urumaco Formation, which is in turn truncated by an Upper Pleistocene terrace (^{14}C date of 20 700 ± 950 years BP at the base) of the Urumaco River. All three outcrops exhibit sharp brittle deformation within the Urumaco Formation, whereas deformation in the overlying alluvial terrace is much more subtle, and is only occasionally detectable (Fig. 3 of Audemard et al., 1999a).
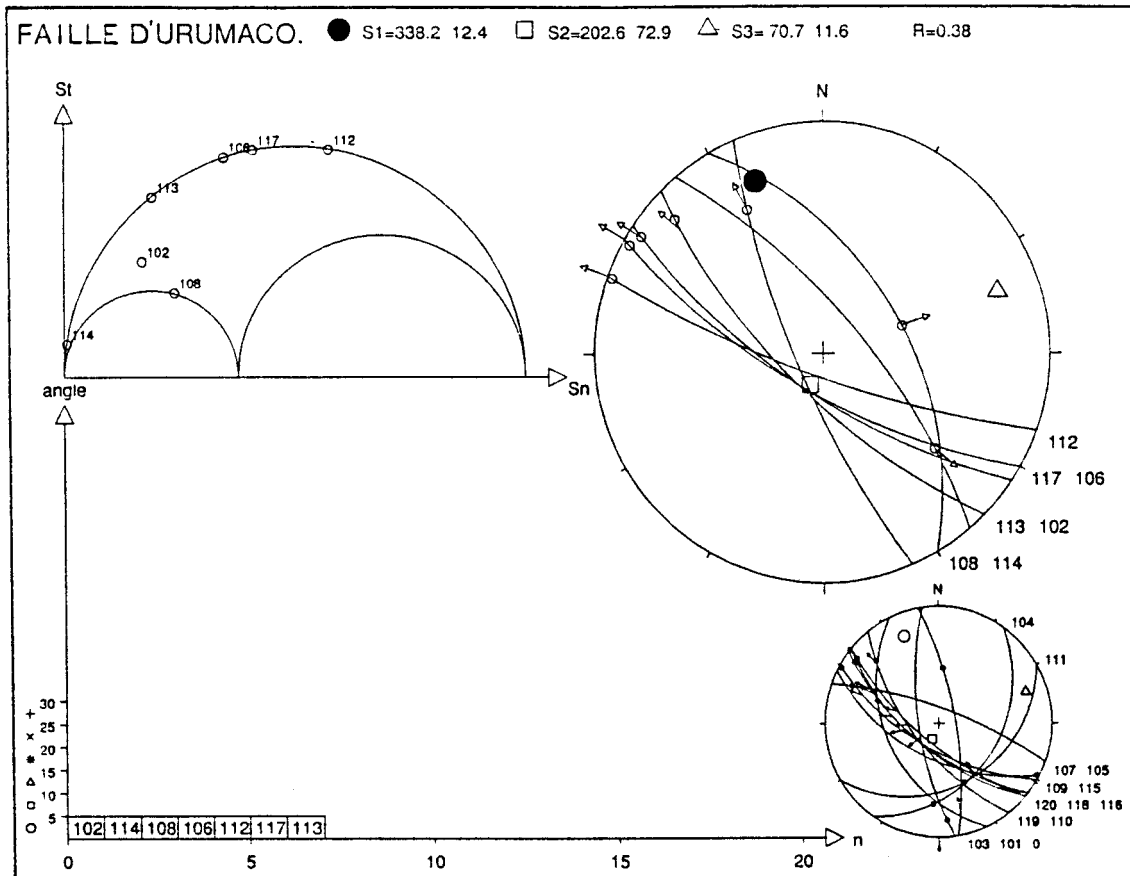
Fig. 4. Stress tensor determination for the Urumaco Fault data set, at the Mamón creek-Urumaco river confluence, by means of the Etchecopar et al. (1981) method (Audemard, 1993). Solution displays clockwise from upper left corner: (a) Mohr diagram where fault planes are represented by open circles; (b) lower hemisphere stereographic projection of fault data set incorporated in the tensor solution; (c) lower hemisphere stereographic projection of unused fault set for this solution; (d) histogram distribution in five degree slices of deviation between measured and calculated striations. All tensor solutions in this paper exhibit the same representation.

A palaeoseismic investigation at the northernmost of these river cuts indicates the occurrence of two moderate magnitude (M ∼5.8–6.4) earthquakes in the last 20 Ka for this eastern segment of the Urumaco Fault (Audemard et al., 1999a). Here, two prominent fault planes occur as a wedge and appear to have had different styles of fault behaviour. The southwestern bounding plane juxtaposes two different sequences, both part of the Urumaco Formation, and exhibits righ-lateral striations. The northeastern plane has no change in stratigraphy across it and shows oblique-slip striations (29°N, normal-right-lateral). As mentioned above, the up-dip prolongations of the planes into the overlying alluvial unit are not distinct. A minor (17 cm) 'throw' of the erosive bottom of the terrace at the southwestern plane is probably an artifact, and most of the apparent fault throw at the top of the Urumaco Formation is due to Quaternary erosion of the highly fractured underlying beds. However, a mud-flat deposit within this unit is offset by 14 cm immediately above the northeastern fault plane, sharply affecting the underlying Miocene unit. The fault-bounded wedge observed on the northernmost outcrop can be traced southeastward through the other two river cuts.

A total of 20 fault planes were measured at the three outcrops. Results of the method of Etchecopar et al. (1981) applied to the fault data set obtained at this locality are poor, since the tensor obtained is strongly conditioned by the fact that a single conjugate transcurrent fault set is present. This tensor is characterized by maximum and minimum principal stresses oriented 331.2° 12.4° and 63.7° 11.6°[1], respectively and R^2 of 0.38, that reflects a transcurrent regime (Fig. 4). Though the resulting tensor may be of poor quality, it is in good agreement with the tensor derived from applying the simple shear model to the large-scale regional structures.

Of the remaining fault planes, no other tensor could be determined because of the small data set. Nevertheless, these data show considerable variability of striation pitch for faults of similar orientation, implying different motions on the Urumaco Fault. Indeed some minor striated faults,

---

[1] A declination of 7° W is to be added to all magnetic orientations.

[2] $R = (\sigma_2 - \sigma_3)/(\sigma_1 - \sigma_3)$ and $\sigma_1 \geq \sigma_2 \geq \sigma_3 \geq 0$, after Etchecopar et al. (1981). R then varies between 0 and 1. This extreme value means that two principal stresses are whether weak or strong, respectively.

subparallel to the Urumaco trend, show left-lateral slip, which is in accord with apparent left-lateral offsets determined from aerial photo interpretation on a short fault strand located near the Mamón creek; this implies that the fault has formerly been activated in an opposite sense (Fig. 3).

5.3. Slip rate

Using two independent approaches (height of flexure due to shortening at the restraining stepover and cumulative coseismic slip at El Mamón paleoseismic site), Audemard et al. (1999a) have bracketed the slip rate of this fault between 0.33 and 0.46 mm/year, about half the rate formerly proposed by Soulas et al. (1987).

6. Río Seco Fault

6.1. Active trace

The onshore trace of the WNW–ESE-striking Río Seco (also named Sabaneta) Fault may be followed for over 20 km, from the northeast of the Río Seco fisherman village to the Mitare River, at about 5 km north of Sabaneta. At its northwestern tip, the fault splays into two strands, the northern one being the longest (Fig. 5). Both strands are easily mappable across the Pliocene San Gregorio Formation because of extensive excellent exposures. Cumulative post-Pliocene right-lateral offset on the northern and southern strands are 620–750 m (measured on a unique *Crassostrea sp* bed) and 30–50 m, respectively. In addition, the main strand also affects Lower Pleistocene (Q_4) pediments uncomformably resting on Pliocene strata. This main fault exhibits 0.5–1 m high, NE-facing, degraded fault scarps in the Pleistocene deposits at several localities (Fig. 5). Other geomorphic indicators of Quaternary activity, generally along the main strand (Fig. 5), include fault trenches, linear and right-laterally-offset drainages, fault benches and saddles. However, fault-line scarps are very common along several minor faults and the two principal strands, since the Pliocene strata are readily exposed by erosion of the upthrown (hanging wall) block.

Along and close to the Río Seco Fault, several other structures are mapped (Figs. 5 and 6). These include: (a) several NW–SE-trending synthetic Riedel shears; (b) occasional nearly north–south-striking antithetic Riedel shears; (c) an ENE–WSW oriented, north-verging thrust fault; (d) a NNW-to-NW-striking fault with dominant normal slip (whose strike lies in the acute angle between conjugate Riedel shears); (e) a subparallel assymetric syncline warping Lower Pleistocene pediments to dips of 27° S and 15° N; and (f) a subparallel double-plunging conical anticline, affecting Neogene strata, within the upthrown block of the fault.

With the exception of the subparallel folding (e and f), all structures associated with the Río Seco Fault match well with a simple shear model (Wilcox et al., 1973). From the derived stress tensor, σ_1 is aligned roughly N140°, and σ_3 is aligned roughly N050°. Taking the folds into account, however, the stress tensor is probably more representative of a compressive-transcurrent regime, implying a stronger obliquity of the maximum horizontal stress with respect to strikes of the fault and fold axial plane; i.e. a NNW–SSE alignment. This subparallel folding had been previously reported by Jaeckli and Erdman (1952) and Méndez and Guevara (1969). The folds are definitely active, as is clear from the northwestern offshore prolongation of the anticline deduced by Graf (1969) based on the present submarine facies distribution of the Mitare Delta (Zeigler, 1964). Recent activity of the Río Seco Anticline is also evident from the cliffed coastline across this structure (Graf, 1969), which contrasts with the low-relief coast elsewhere along western Falcón.

The geometries and locations of both brittle and ductile active structures manifest at the surface match well with available seismic profiling interpreted by Audemard (1993; refer to fig. 4.7). The seismic profiles reveal the following important characteristics, from the northeast to the southwest. First, in the northeast the main Río Seco Fault has a significant reverse component where the north block is downthrown; this is consistent with both the degraded NE-facing scarps of Quaternary age and preservation of the Lower Pleistocene pediments on it, and is in addition to the right-lateral component determined from geomorphic features (Fig. 6). Second, this vertical slip component conflicts with the observation that Neogene thickness of the upthrown block is twice that of the downthrown block, confirming the suggestion by Boesi and Goddard (1991) that recent tectonic inversion has taken place. The inversion of the Urumaco Trough, which is bounded to the north by the Río Seco Fault, may be related either to the present kinematics of the right-lateral Oca–Ancón Fault (Audemard, 1993) or to simple Quaternary transpression along the Río Seco Fault. Third, the assymetry of the Quaternary syncline corresponds to the general geometry of the underlying structure in Neogene sedimentary rocks, characterized by a gentle southwest limb and a steeper northeast limb.

The Río Seco Fault appears to extend northwestward into the Venezuela Gulf shelf, possibly as far as the Cuiza Fault (Beltrán, 1993) which outcrops in the Goajira Peninsula; further studies are needed to confirm this. To the southeast, the fault may kinematically transfer slip either to the north–south-trending Mitare Fault, supposedly a left-lateral structure, or to the ENE–WSW-striking Guadalupe-Chuchure Thrust. Linkage with the thrust fault seems more likely, since localized compression induced at the fault tip could be reduced by right-lateral slip along the Río Seco Fault.

6.2. Microtectonics

Two microtectonic stations were recorded on the Río Seco Fault: one at the northwesternmost portion of the fault (corresponding to the previously described area), and
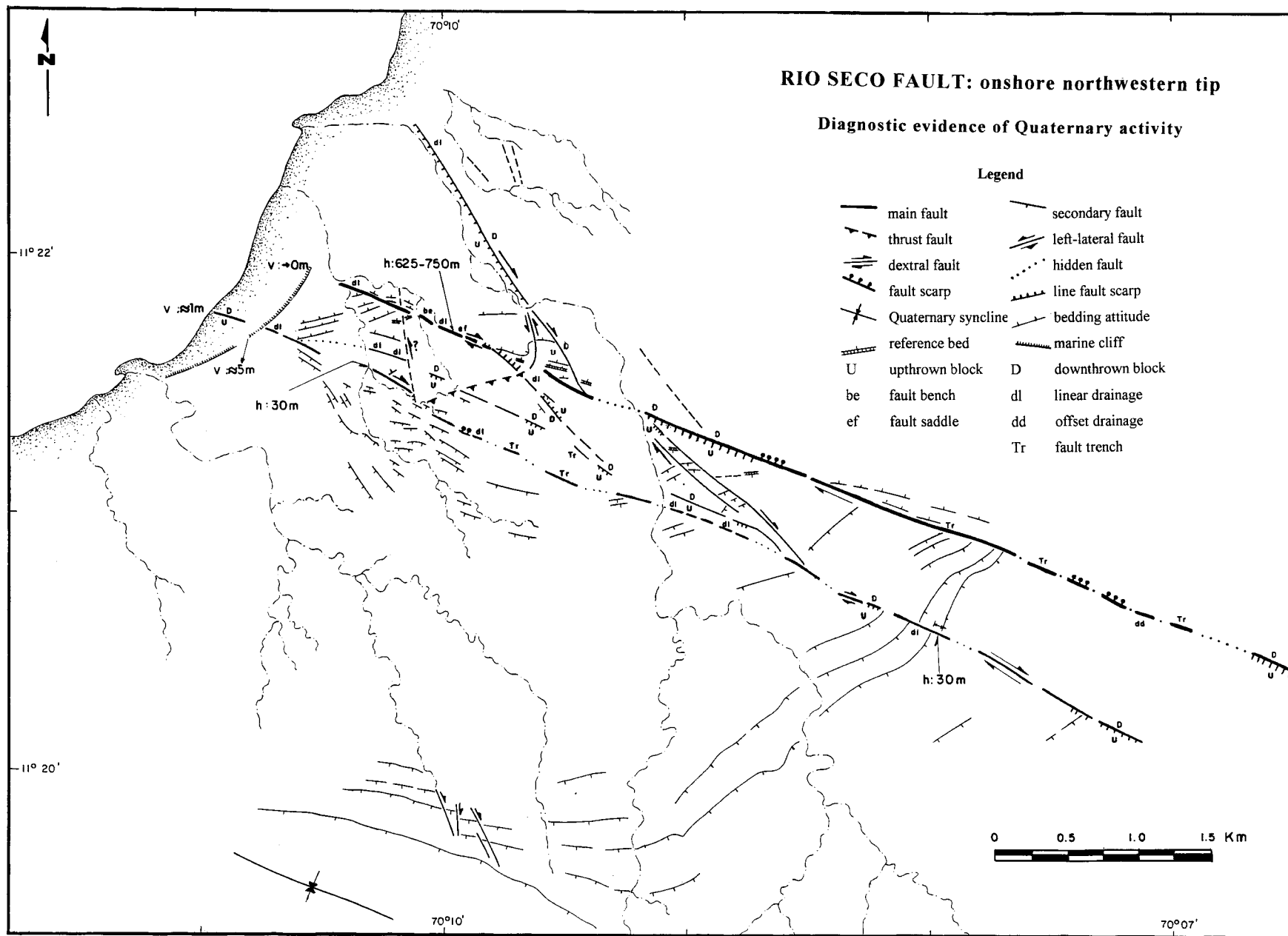
RIO SECO FAULT: onshore northwestern tip

Diagnostic evidence of Quaternary activity

Legend

——	main fault		secondary fault
	thrust fault		left-lateral fault
	dextral fault		hidden fault
	fault scarp		line fault scarp
	Quaternary syncline		bedding attitude
	reference bed		marine cliff
U	upthrown block	D	downthrown block
be	fault bench	dl	linear drainage
ef	fault saddle	dd	offset drainage
		Tr	fault trench

70°10'

11° 22'

v : →0m

v :≈1m

v :≈5m

h:625-750m

h : 30m

11° 20'

h: 30m

70°10'

70°07'

0   0.5   1.0   1.5 Km

Fig. 5. Conventional geologic and neotectonic mapping of the northwestern termination of the Río Seco Fault traces onshore (Audemard, 1993).
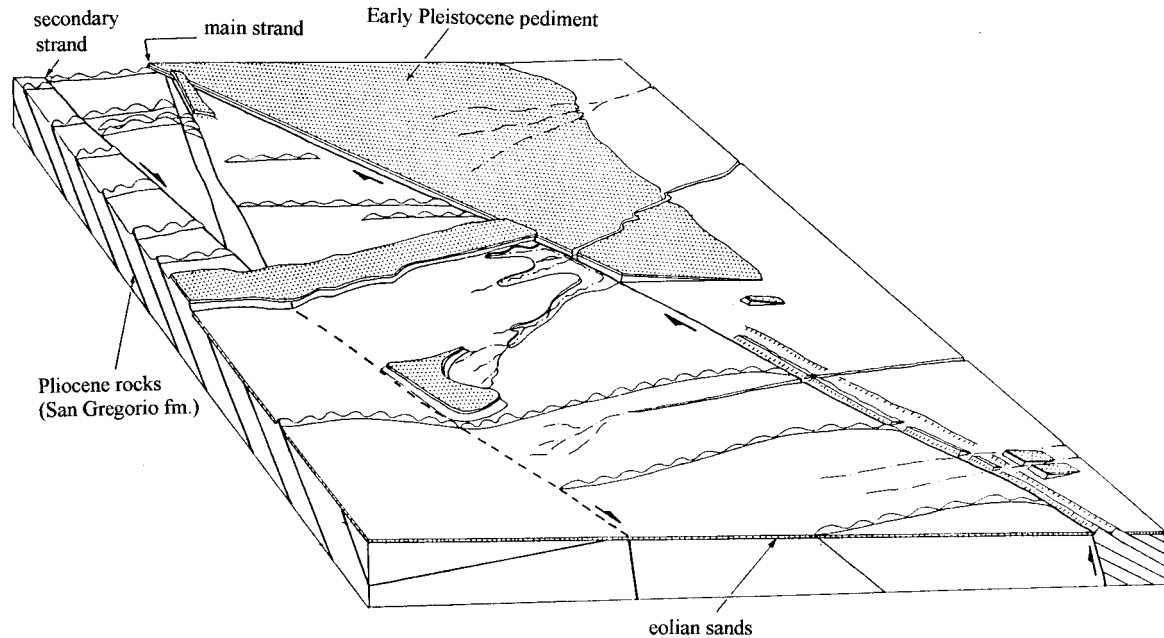
Fig. 6. Block diagram displaying the central portion of the northwestern termination of the Río Seco Fault shown in previous figure (Audemard, 1993).

a second station at the opposite end, near the Mitare river (Figs. 1 and 3 inset).

6.2.1. Río Seco exposure

The northwestern onshore termination of the Río Seco Fault trace exhibits intense brittle deformation of the Upper Pliocene San Gregorio Formation (Fig. 5). Here, fault planes commonly are underlain by or infilled with gypsum fiber growth that allow precise determination of the sense of slip (Fig. 7a–d). Occasionally, sigmoidal tension gashes show two different generations of gypsum fiber growth; both syntaxial (Fig. 7a and c) and antitaxial (Fig. 7b). Sixty-five fault plane determinations (fault plane attitude, striae pitch and fault slip; offsets when possible) were measured at this locality, the second largest micro-tectonic data set recorded in the northern Falcón. Some fault planes reveal two superposed striation generations; in two cases, the pitch varied but the sense of motion was preserved. In another case, continuous curved striations imply that fault kinematics progressively changed through time (Fig. 7d) between left-lateral reverse (pitch of 67° N) and reverse right-lateral (pitch of 15° S). Most structural data were collected between two main fault strands, so block rotation could explain the presence of curved striations (Fig. 7d).

Determination of stress tensors at this station through the Etchecopar et al. method was very satisfactory. Four solutions were obtained by progressive discriminations of those faults satisfying a tensor (Fig. 8):

1. The first tensor, which accounts for the 45% of the entire fault data set, is characterized by: σ_1: 350.0°, 9.5°; σ_3: 257.3°, 15.7°; $R = 0.20$ (Fig. 8a). This tensor corresponds

to a compressive-transcurrent regime with a maximum horizontal stress oriented NNW–SSE. This solution is of good quality, though faults labelled 140 and 150 may not comply with the friction law.

2. The second stress tensor, representing 15% of the fault population data, is aligned: σ_1: 8.2°, 19.7°; σ_3: 102.4°, 11.0°; and R is 0.34 (Fig. 8b); again, this indicates a compressive-transcurrent regime. According to the quality criteria proposed by Ritz (1991), this solution is good. This tensor is similar to the previous one but exhibits a small clockwise rotation, which could be explained by the simple shear couple that would impose the two right-lateral strands to the block inside.

3. The third tensor, also accounting for 15% of the entire fault data set, is characterized by: σ_1: 356.2°, 0.2°; σ_3: 100.5°, 89.9°; and R is 0.60 (Fig. 8c); this indicates a compressive regime. Location of several measurements near the abscissae axis in the Mohr circle (fault planes of low τ/σ_n ratio) is coherent with a compressive regime but, since these do not obey the friction law, the validity of this tensor is debatable.

4. The fourth stress tensor, which accounts for only 10% of the data set, is oriented: σ_1: 125.2°, 15.2°; σ_3: 218.6°, 12.2°; and R is 0.54 (Fig. 8d); this characterizes a transcurrent regime. Based on the quality criteria of Ritz (1991), this solution seems skewed by fault plane 131, implying that it may not be reliable.

No other solution arose from the remaining 15% data set, which instead may reflect complex block rotations.

6.2.2. Mitare river exposure

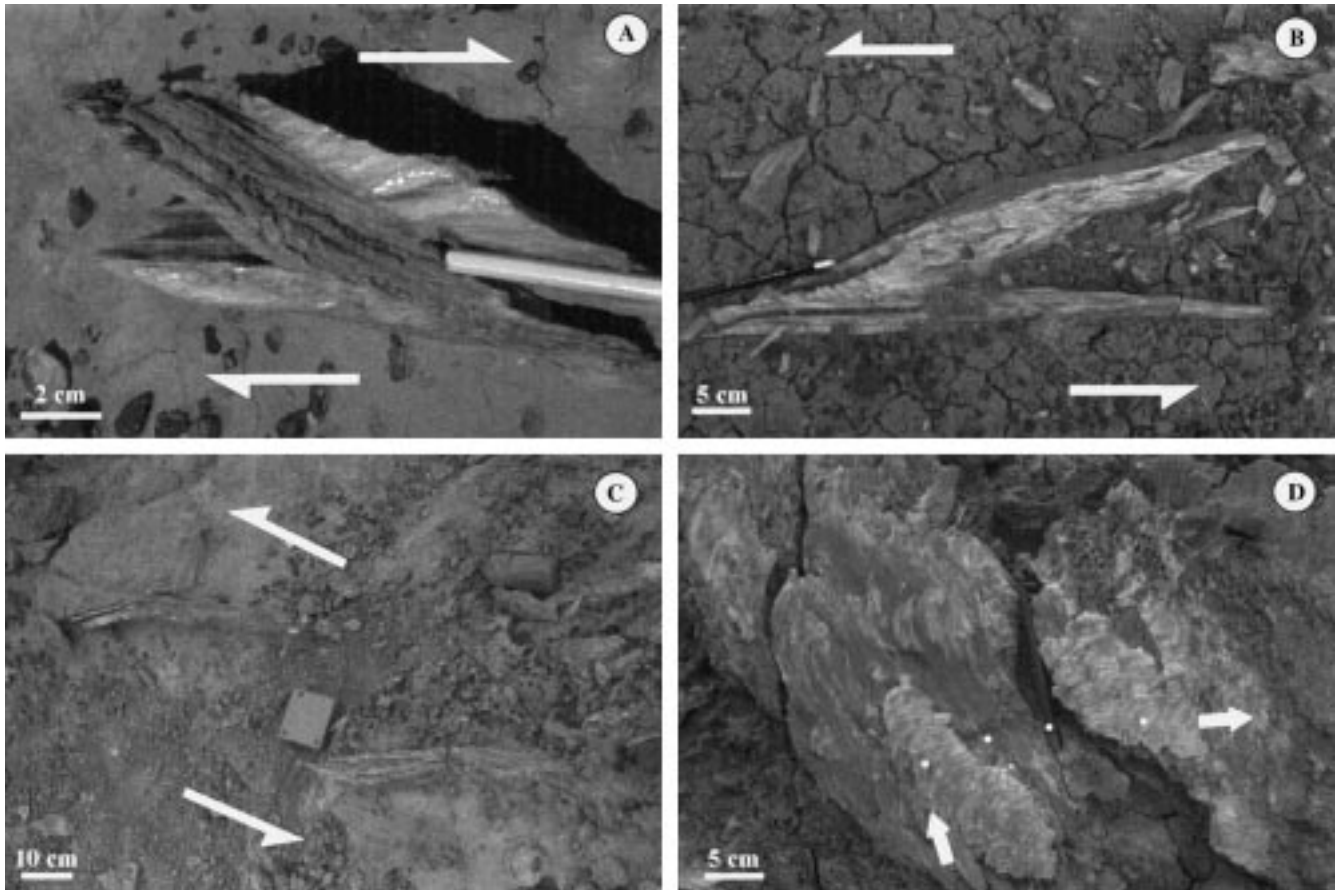At the southeastern end of the Río Seco Fault near the

Fig. 7. Gypsum fiber growth has been a useful tool for determining slip sense along the Río Seco Fault. Several mesoscopic features are shown: (A) several generations of syntaxial fiber growth; (B) antitaxial fiber growth in sigmoidal tension gash that denotes left-lateral sense of slip (fault attitude: N 020° 86° W; striation pitch: 30° N) and (C) sintaxial fiber growth in en echelon sigmoidal tension gashes; (D) curved striations on some fault surfaces (follow dots between arrows) indicate block rotation, which could account for shear coupling introduced by two subparallel strands of this fault.

Mitare river, some 5 km north of Sabaneta (Fig. 3 inset), fault plane data were collected from a conglomerate bed (oriented at N 130° 33° N) of the Upper Pliocene San Gregorio Formation. Due to the coarse lithology, only nine striated planes were characterized. Nevertheless, a stress tensor was calculated with the following attitudes: σ_1: 323.3°, 30.5°; σ_3: 193.0°, 47.7°; R is 0.24 (Fig. 9). After counter-tilting the tensor to counteract the bedding dip, the corrected attitudes are σ_1: 338°, 20°; σ_3: 150.0°, 71°; this indicates a compressive-transcurrent regime.

6.3. Slip rate

Based on the 620–750 m and 30–50 m right-lateral offsets of Upper Pliocene beds of the San Gregorio Formation measured across the main and secondary strands respectively, an average slip rate of 0.34 ± 0.03 mm/year and 0.020 ± 0.005 mm/year may be deduced for the respective strands (Audemard, 1993). Consequently, the cumulative right-lateral slip rate is about 0.36 ± 0.03 mm/year. However, it might be slightly higher because the secondary vertical (reverse) component has been neglected for this estimation (Audemard, 1993).

7. Taima–Taima Thrust

7.1. Active trace of the thrust

The Taima–Taima (or Guadalupe) Thrust is the north-easternmost segment of a major thrust that extends onshore westward for about 60 km from the town of Puerto Cumarebo to the village of Las Piedras (Audemard, 1993), located south of Sabaneta (Fig. 10; relative location in Fig. 1). This major thrust fault is assigned different names along strike from east to west Guadalupe, Mina de Coro and Chuchure because its trace is not continuous. This structure essentially lies at the boundary between the positive relief of the Falcón Range and the low-lying coastal plain of northern Falcón State. The fault trace has been established by conventional geological mapping since it has little or no geomorphic expression. However, Pliocene and Pleistocene
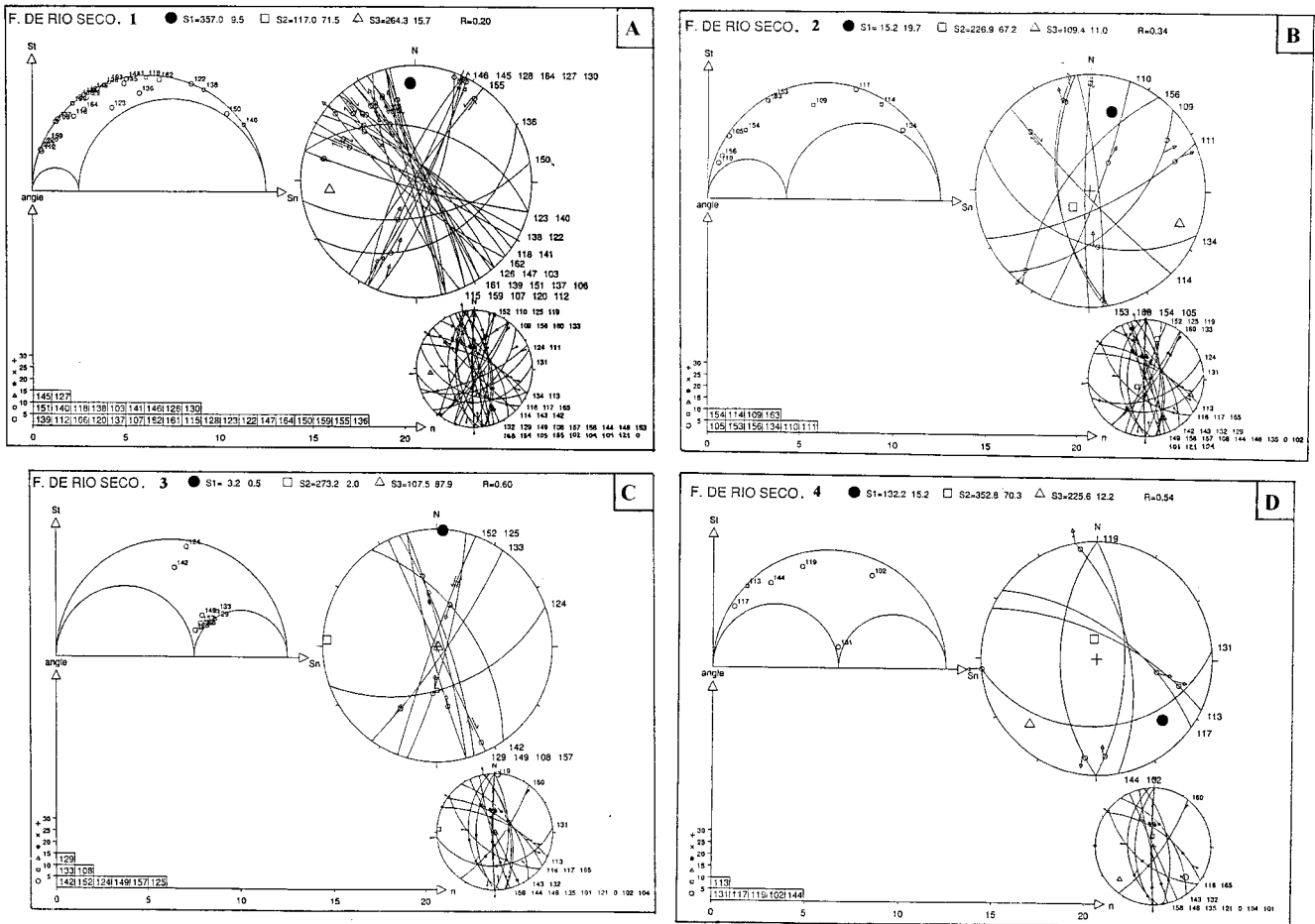
Fig. 8. Stress tensor determination for the Río Seco Fault data set, at the onshore northwestern termination (see Fig. 3 inset and Fig. 10 for relative location), by means of the Etchecopar et al. (1981) method (Audemard, 1993). Four stress tensor solutions are shown (see text for discussion).
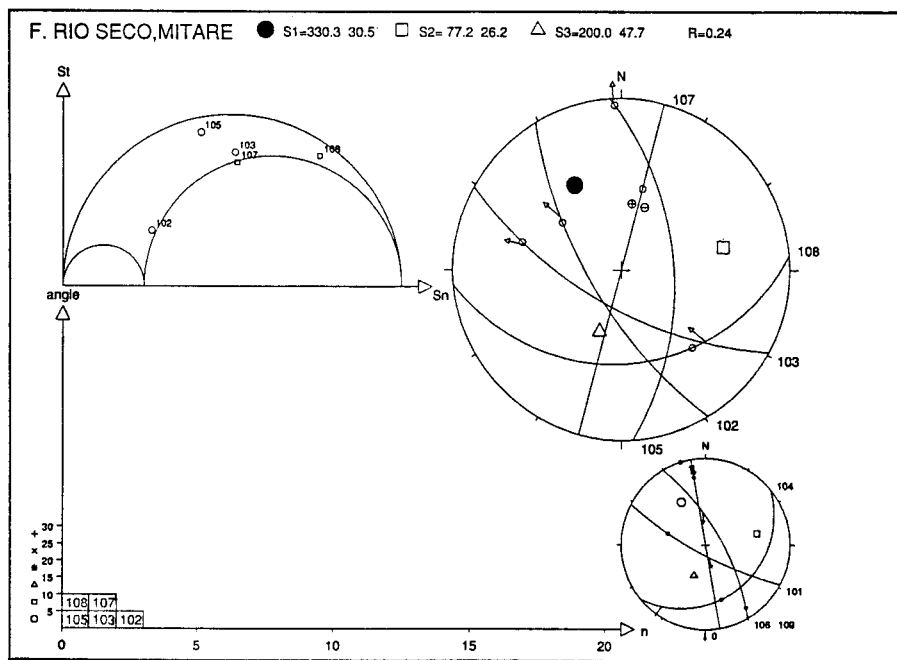

Fig. 9. Stress tensor determination for the Río Seco Fault data set, near the Mitare River (see Fig. 3 inset and Fig. 10 for relative location), by means of the Etchecopar et al. (1981) method (Audemard, 1993). Solution display is the same as for Fig. 4.

Fig. 10. Neotectonic map of the Paraguaná Peninsula and Coro surrounds (after Audemard, 1993), showing main active tectonic features. Legend as Fig. 3.
Additional legend: solid arrows indicate age of youngest deformed geologic markers whereas empty arrows correspond to age of sealing marker.

units are offset or tilted at several localities (Fig. 10) and its vertical throw has been estimated at 300 m (Ferrell et al., 1969).

At two locations along its complex trace, the front of this major thrust fault jumps south by up to 10 km because of short left-lateral (tear) faults or complex zones. One 'jump' occurs east of Coro. Here, between the villages of La Vela and Caujarao, the front switches southward from the southern Carrizal fault tip to a steep, north-dipping monocline affecting Upper Pliocene-Lower Pleistocene fanglomerates (the Coro Formation) (Fig. 10). Along this zone, the thrust plane does not crop out, but is instead manifest as a set of NE–SW-trending 'en échelon' folds (Audemard, 1993) (Fig. 10). This geometry, and the associated structures, suggests it is a transfer zone, similar to those described by Baby et al. (1993) and Calassou et al. (1993). Analogue sand-box modelling of this configuration (Audemard, 1993; Audemard and Calassou, 1996) indicate the presence of a down-to-the-east basement step oriented perpendicular to the northward vergence of the thrust.

Further west, this major thrust system has been located by Wiedenmayer (1937) between Caujarao-El Isiro and San Antonio, southwest of Coro. At La Mina de Coro, an ancient abandoned coal mine, the Middle Miocene Cerro Pelado Formation is overthrusted onto the Upper Miocene Caujarao Formation.

The second 'jump' of the front occurs at the western end of this segment (Fig. 10), where the San Antonio Fault (Wiedenmayer, 1937) or Hatillo Fault (Cross, 1952) offsets it left laterally by as much as 2.5 km, though the post-Pliocene (post-La Vela Formation) displacement being less than 1 km. Further west, between San Antonio and Sabaneta, the thrust fault is inferred by the Creole company map (Bellizzia, 1971) to be located south of la Fila Capote within the mudstones of the Middle Miocene Querales Formation; consequently it has no geomorphic expression. Cross (1952) had mapped exactly the same thrust fault trace, which he named Chuchure, between Las Piedras (slightly south of the village of Sabaneta) and San Antonio (southwest of Coro), along the valley of the small village of Chuchure (Fig. 10). Cross mentions that the northern block corresponds to a north-dipping monocline, whereas the southern block is intensively deformed by faults and folds, some of which are overturned. He interpreted the Chuchure structure as a north-verging, steeply dipping reverse fault.

The Guadalupe (or Taima–Taima) segment of this major thrust front lies mainly offshore, but the La Vela Anticline in its hanging wall is exposed along the coast close to the town of La Vela de Coro (Fig. 10). The geometry of the La Vela anticline is rather well known, based on detailed borehole studies by González de Juana in the 1930s and recent seismic profiling (Audemard and De Mena, 1985 and Cabrera de Molina, 1985). These show the fold to be a brachy-anticline (i.e. length and width are nearly the same), with its longest axis trending N070° to N080°. The anticline is bounded to the west by the left-lateral Carrizal Fault,

which strikes N010° to N015°. To the east, it is bounded by a NW–SE-trending system of faults that controls the eastern coast of the Falcón State, and which includes the La Soledad and Santa Rita faults (Figs. 1 and 10). González de Juana (1937), González de Juana (1972) and Kavanagh de Petzall (1959) originally interpreted the La Vela structure as a brachy-anticline with two double-plunging anticlinal axes trending N070° to N080°, separated by a very narrow sub-parallel syncline, where the main south-located anticline is gently folded, whereas the northern anticline has a vertical-to-overturned northern limb. A re-interpretation by Audemard (1993) considers that the main gently folded dome is partially separated from the northern narrow overturned anticline by thrust fault that is sub-parallel and secondary to the main Guadalupe (Taima–Taima) Thrust. Based on seismic profiles (Audemard and De Mena, 1985 and Cabrera de Molina, 1985), the dip of the Guadalupe thrust plane is about 30° to the south, very similar to the dip represented on a geological cross-section of La Vela Anticline interpreted by González de Juana (1937). The sedimentary sequence involved in this folding ranges in age between Middle to Upper Miocene (Socorro and Caujarao formations) and Pliocene (La Vela Formation). The shallow inner-shelf marine sediments of the La Vela Formation are perfectly upright west of El Muaco pier and the Carrizal Fault, implying that fault-related folding has been ongoing during the Quaternary. Strong differential uplift can also be inferred by the present juxtaposition of the onshore relief of La Vela Anticline from the offshore seaboard of the Guadalupe Thrust. Direct evidence of this coastal thrust-related uplift of La Vela Anticline is the occurrence of a 2700-year-old, 1.5-m-uplifted beachrock on the northern limb of this fold, east of the Muaco pier (Audemard et al., 1997).

Due to lack of reliable offsets in Quaternary surface markers, slip rate of the Taima–Taima Thrust fault was derived from subsurface data, yielding a value of 0.1 mm/year (Audemard, 1993).

7.2. Microtectonics

Microtectonic analyses were undertaken at two localities along the trace of this thrust. There were: (1) slightly north of Caujarao, along the Coro-Caujarao road; and (2) at Puente de Piedra (Coro-Puerto Cabello national road), south of the gently domed main body of La Vela Anticline. In addition, some fault plane determinations were also made along the north–south-striking Hatillo (or San Antonio) Fault; although left-lateral strike-slip was confirmed from drag folds, no stress tensor determination could be made because fault-plane data set revealed strong rotation and tilting.

7.2.1. Caujarao exposures
Artificial cuts along the Coro-Caujarao road or abandoned gravel pit walls expose fanglomerates of the Plio-Pleistocene Coro Formation, the stratotype locality of this unit (Vallenilla, 1953). The strata define a steep
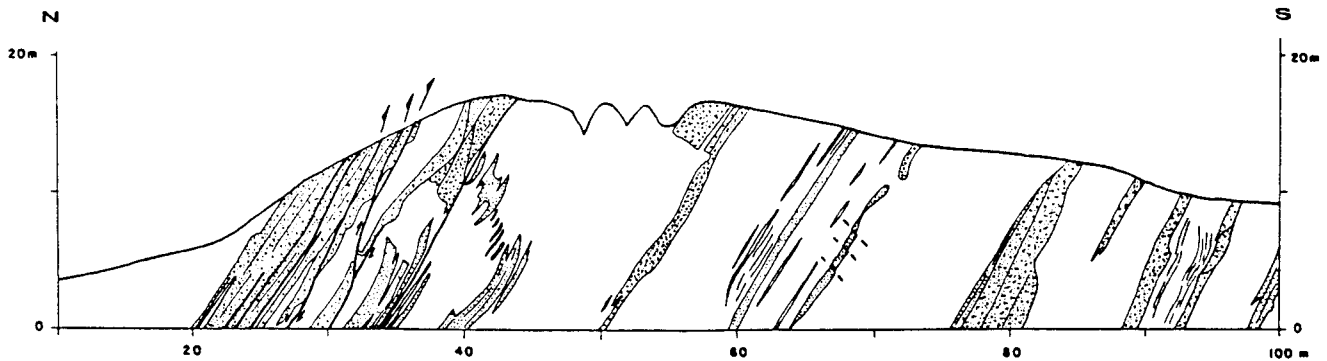
Fig. 11. Log of west-facing road cut, at the stratotype locality of Caujarao and Coro formations, where some fanglomerate beds of the Pliocene Coro Formation are faulted (after Audemard, 1993). Notice slight obliquity between faults and bedding planes.

north-dipping monocline (Fig. 11), which forms part of the northern limb of an assymetrical anticline. The relationship of the Coro Formation with the underlying sedimentary units is still a matter of discussion. For instance, Vallenilla (1953) indicates that the Coro Formation lies conformably on La Vela Formation, but then contradicts this by showing a 7° dip difference between those two units (Vallenilla, 1961). Jaeckli and Erdman (1952) and Wozniak and Wozniak (1979) agreed on the unconformity between both units, but Graf (1969) contended that the Coro Formation is conformable on La Vela Formation but is uncomformable on older sedimentary rocks. Audemard (1993) believed the debate could be resolved if both units were separated by a progressive unconformity, but this could not be firmly established from the field evidence.

With the exception of steep (65–70° N) bedding in the fanglomerates, the only deformation structures visible at outcrop scale are a few subvertical faults oriented slightly oblique to stratification (Fig. 11 and fig. 4.37 in Audemard, 1993). Kinematic indicators on those fault surfaces, together with some small drag folds, established the reverse character of these faults (Fig. 12). However, striated fanglomerate bedding surfaces also testify to flexural-slip folding. In addition, cobble surfaces of the conglomerate beds are frequently striated. These observations suggest that this fanglomerate sequence was incrementally tilted northwards during a single tangential phase. Initial shortening probably induced small thrust faults slightly oblique to the sub-horizontal bedding. Following this, horizontal compression tightened folding progressively by flexural slip, probably in association with a north-verging thrust fault (an early fault-propagation fold). Consequently, the northern limb of the assymetrical anticline progressively acquired an increasingly steeper northward dip. Finally, the anticline may have evolved into a faulted fold, as is clear west of Caujarao, at Mina de Coro, where the core is thrust-faulted. This interpretation has significant implications for the stress tensor determination based on the microtectonic assessment of this locality.

This group of outcrops produced the largest of the kinematic data sets from the Falcón Basin, with 140

measurements of fault-plane attitude and sense of slip. Most of the measurements were recorded from striated convex cobble surfaces. Taking into account that those surfaces are potential discontinuities where sliding may take place (Schrader, 1988; Taboada, 1993), conglomerates are an ideally pre-fractured medium (Combes, 1984; Casagrande Fioretti, 1985). These conglomerates have almost no matrix, making it unlikely that any cobble rotation may have occurred.

Six stress tensors have been calculated by successive discrimination of those faults already satisfying a tensor (Fig. 13). Their characteristics are summarized in Table 1. Several comments may be made of these tensors. First, regardless of the variability of measured fault-plane orientations, a large portion of them are sub-parallel to bedding plane and conform to bedding surface striations. Second, maximum stress for all but one of the tensors is not contained in the equatorial plane of the stereographic projection, i.e. they are not horizontal. Third, the distribution of fault planes in the Mohr diagrams is satisfactory for all tensors. However, some fault planes corresponding to strilolites (slickolites) appear not to comply with the friction law (very low τ/σ_n ratio), and other fault planes show very high τ/σ_n ratios, corresponding to those displaying calcite recrystallizations at steps. Fourth, several fault planes with dips less steep (~45°) than the sedimentary sequence, exhibit apparent normal dip-slip. Since the sequence is strongly tilted, it seems very likely that they are actually overturned reverse faults.

Given the very steep dip of the Coro Formation fanglomerates at this locality, it seems clear that the stress tensors are probably tilted by up to as much as the sequence itself. Consequently, we counter-tilted all tensors, with the exception of the one already exhibiting a horizontal maximum stress. The amount of applied countertilt was bracketed between the original plunge of σ_1 for each stress tensor and the maximum tilt undergone by the sedimentary sequence. If the applied assumption is correct, the relative chronology suggests that tensor one is the most recent and tensor six is the oldest (Table 1).

From Table 1 and Fig. 14, the following points emerge.

Fig. 12. Small drag fold (identified by a white hexagon) indicates reverse sense of slip of a steeply dipping fault (identified by small arrows) observed on the eastern cut of the Coro-Caujarao road, south of Coro.

(1) The maximum horizontal stress of all tensors gather around the north–south direction (N350° ± 21°). (2) The intermediate and minimum stresses are all contained in the bedding plane ($\overline{S}$ of Fig. 14). (3) All six calculated stress tensors characterize a compressive-transcurrent to compressive regime, with the latter being the most common. (4) The age of tilting (or folding) is younger than deposition of the Plio-Pleistocene Coro Formation, since no intraformational disturbances have been observed and some degree of compaction (but not lithification) is needed for development of pebble striations.

7.2.2. Puente de Piedra

Along the Coro-Puerto Cabello national road, between the villages of Taratara and Puente de Piedra, a 300-m-long road outcrop exhibits a faulted detritic sequence belonging to the Mio-Pliocene La Vela Formation (fig. 4.43 in Audemard, 1993). The strata trend roughly east–west and dip about 40° to the north. The main brittle structure is a thrust fault with a throw of about 1 m (Fig. 15). The thrust plane is slightly oblique to stratification and is associated in the footwall by an antithetic, conjugate thrust fault family. These secondary faults also accommodate some

right-lateral slip, but the pitch of striae is generally over 70°. The general sedimentary and tectonic characteristics suggests that the sequence has been tilted as a single unit (Fig. 15).

At the far eastern end of this road cut, a marine deposit ascribed to the Plio-Pleistocene Coro Formation by González de Juana (1972) lies unconformably on the Mio-Pliocene La Vela Formation, which here strikes north–south and dips at 12° east. The base of the deposit corresponds to a shallow marine (inner shelf) environment, due to faunal content and bioturbation. However, its upper part comprises very fine sands that are very thinly laminated and which could be an older dune generation deposited some time in the Middle to Lower Pleistocene (see Audemard, 1996a, for discussion).

At this outcrop, the microtectonic characteristics of nine faults were recorded. The calculated stress tensor is aligned as follows: σ_1: 346.2°, 17.2°; σ_3: 202.3°, 69.1°; (R is 0.45) (Fig. 16); the R-value indicates a transcurrent-compressive to compressive tectonic regime. Because the whole sequence was tilted, the stress tensor was countertilted by as much as the plunge value of σ_1, implying that La Vela sequence was already partly tilted (12° N) and unfaulted. Besides, any later tilting has to be imputed to this stress
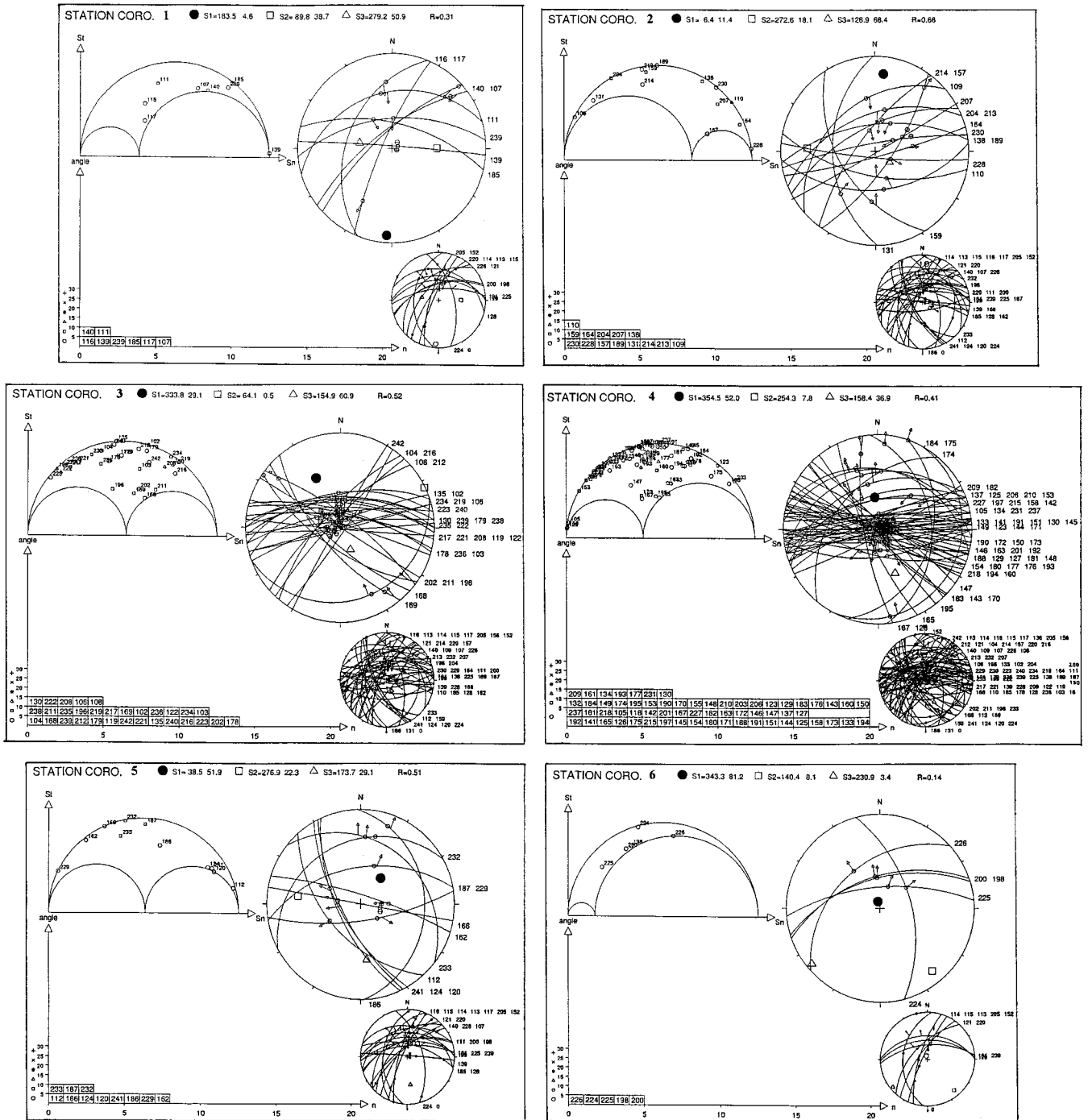
Fig. 13. Stress tensor determination for cobble and bedding striation data set, at the stratotype locality of Caujarao and Coro formations, south of Coro (see Fig. 10 for relative location), by means of the Etchecopar et al. (1981) method (Audemard, 1993). Six stress tensor solutions are shown (see text for discussion). Same representation as for previous tensor solutions.

tensor. The corrected orientation of the principal stresses are: σ_1: 003°, 00° (almost north–south) and σ_3: 324°, 84°.

8. Paraguaná Peninsula

The Paraguaná Peninsula in northern Falcón state comprises rather flat lowlands surrounding the protruding 'inselberg' of Mesozoic igneous-metamorphic complex of the Cerro Santa Ana, upstanding since Oligocene times. The lowlands of this peninsula have mainly developed on top of the Pliocene Paraguaná Formation, which in turn rests uncomformably upon the Santa Ana complex and Miocene sedimentary units. In general, the topography of the

Table 1
Stress tensors calculated from cobble striations in the Coro Formation, at Caujarao, South of Coro.

Tensor label	Number of faults	Stress orientations		Rapport	Imposed angle of rotation	Untilted (rotated) stress tensor	Tectonic regime
		(Undeclined north)	(Corrected north)				
1	8	σ_1: 183.5° 04.6° σ_3: 279.2° 50.9°	σ_1: 176.5° 04.6° σ_3: 272.2° 50.9°	0.31	0°	σ_1:176.5° 04.6° σ_3:272.2° 50.9°	Transcurrent compressive
2	14	σ_1: 006.4° 11.4° σ_3: 126.9° 68.4°	σ_1: 359.4° 11.4° σ_3: 119.9° 68.4°	0.68	11°	σ_1: 003° 00° σ_3: 098° 76°	Compressive
3	31	σ_1: 333.8° 29.1° σ_3: 154.9° 36.9°	σ_1: 326.8° 29.1° σ_3: 147.9° 36.9°	0.52	29°	σ_1: 329° 00° σ_3: 061° 82°	Compressive
4	63	σ_1: 354.5° 52.0° σ_3: 158.4° 36.9°	σ_1: 347.5° 52.0° σ_3: 151.4° 36.9°	0.41	52°	σ_1: 345° 00° σ_3: 067° 80°	Transcurrent compressive
5	11	σ_1: 038.5° 51.9° σ_3: 173.7° 29.1°	σ_1: 031.5° 51.9° σ_3: 166.7° 29.1°	0.51	62°	σ_1: 011° 00° σ_3: 303° 88°	Compressive
6	5	σ_1: 343.3° 81.2° σ_3: 230.9° 03.4°	σ_1: 336.3° 81.2° σ_3: 223.9° 03.4°	0.14	70°	σ_1: 343° 10° σ_3: 247° 20°	Compressive transcurrent
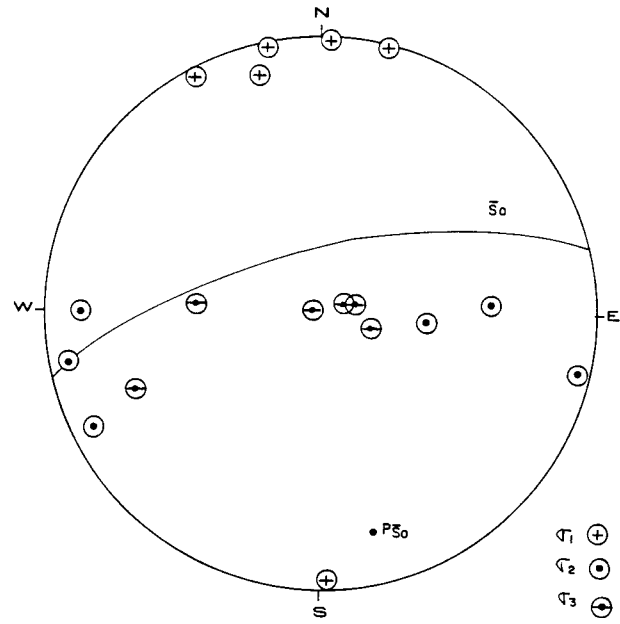
Fig. 14. Lower hemisphere stereographic projection of all six stress tensors calculated by means of the Etchecopar et al. (1981) method (Audemard, 1993), at the Coro-Caujarao microtectonic evaluation site, after counter-tilting (see text for explanation).

lowlands corresponds well to underlying structure due to the competence of the top member of the Paraguaná Formation, a well-indurated fossiliferous marine limestone.

Although fault-controlled, the Paraguaná Peninsula has long been considered a tectonically stable block during the Andean orogeny (Feo-Codecido, 1971). However, the recognition by Danielo (1976) of four marine terraces (at +80 m, +40–50 m, +15–20 m, and +6 m) argued against such stability. The terraces are mainly marine erosional surfaces that truncate the top member of the Pliocene Paraguaná Formation. In addition to the present-day marine deposits, patches of correlative marine sediments can be mainly observed associated with the two terraces closest
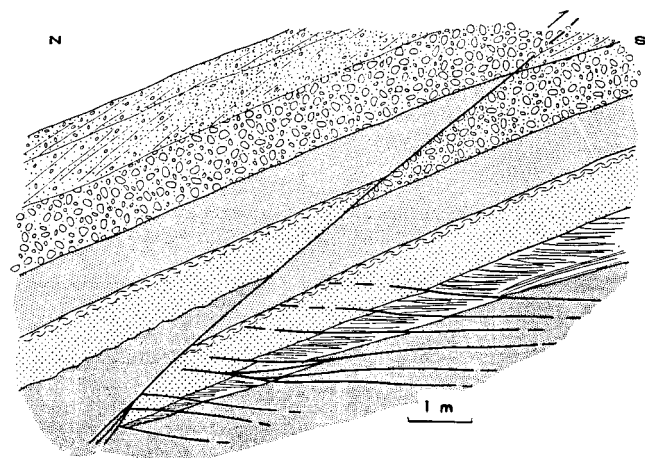

Fig. 15. Conjugate thrust fault system at the Puente de Piedra outcrop. Notice that both sequence and fault system are north-tilted.
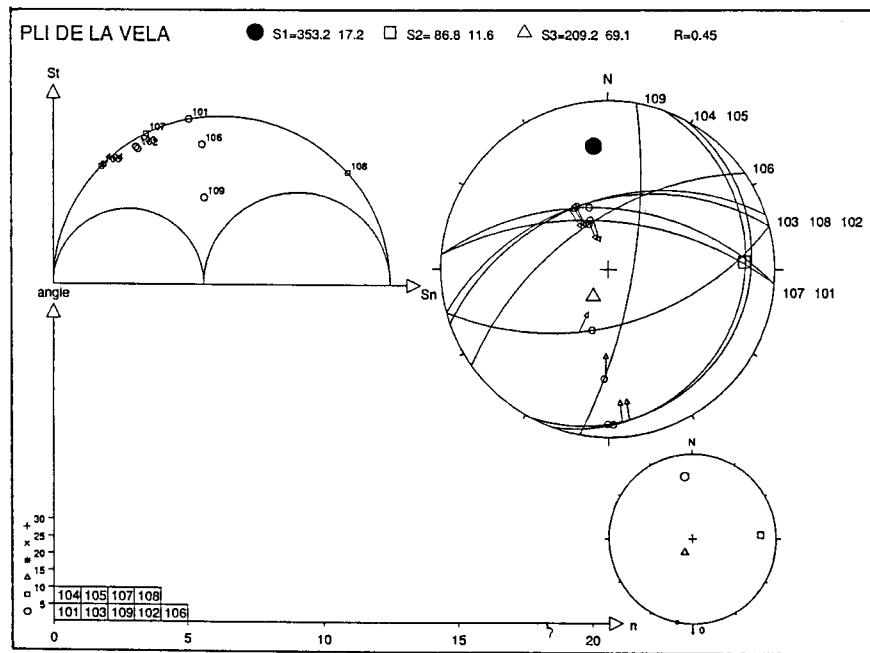
Fig. 16. Stress tensor determination for the Puente de Piedra conjugate thrust fault system, by means of the Etchecopar et al. (1981) method (Audemard, 1993).

to sea level. Consequently, there is no proof of an undoubted marine origin for the two higher terraces, except for the El Alto Conglomerate associated with the third highest terrace on the eastern (windward) side of Paraguaná. Although Graf (1969) reported marine patches correlable to these marine abrasion surfaces, Audemard (1996a) suggested that the terraces may have originally been cut by marine erosion but later reworked by subaerial erosion, thereby explaining the lack of any marine remnant deposition. Based on the assumption by Danielo (1976) that the oldest terrace is Lower Pleistocene in age, we derive an estimate of < 0.08 mm/year Quaternary uplift rate for the Paraguaná block, confirming general tectonic instability during the Quaternary (Audemard, 1993). Such a low uplift rate would be in agreement with the present strike-slip tectonic regime in northwestern Venezuela (Audemard, 1993, 1997), where only small vertical motions should be expected.

Evidence of Quaternary tectonic activity has been identified at several outcrops located around the margins of the Paraguaná Peninsula (Fig. 10) (Audemard, 1993; 1996a,b). The key sites, following the coast clockwise from the west are: Los Taques-Punta Salina, Punta Macolla, Cabo San Román and around Las Cumaraguas. The timing of folding and/or faulting at these localities is bracketed between the age of lithification of the Pliocene Paraguaná Formation and before the erosion and deposition of a terrace tentatively ascribed to oxygen isotope stage 5 highstands. This roughly places the bulk of the deformation in the Paraguaná Peninsula in the Lower to Middle Pleistocene. However, one exception is likely to be the latest activation on the Cabo San Román and Puerto Escondido Faults, which may be

Upper Pleistocene to Holocene in age (for more details, refer to Audemard, 1996a,b). Although beyond the scope of this paper, some aspects of the neotectonic deformation of the peninsula are important for the discussion of the stress history of the region.

Along the western Paraguaná coast, the Punta Cardón–Punta Salinas section (southern segment of this coast) features high cliffs that are cut into the Pliocene Paraguaná Formation and which may be indirect evidence of vertical tectonics. This cliffed coastline may be split into two sections. The first is the southern section, between Punta Cardón and Astinave (dry dock north of Amuay), where cliff erosion is still active and where the greatest water depth is found (Fig. 10). The second is the northern portion, between Astinave and Punta Salinas, where the cliffs are relict and are separated from the seashore by a salt-flat or mud-flat and later a barrier beach. The maximum height of these cliffs is about 20 m high, and is found roughly in the middle at Punto Fijo, declining in height progressively to both ends and displaying an apparent smooth dome-like structure at the top member of the Paraguaná Formation. This dome-like structure might simply reflect the radial outward dip from the Santa Ana Complex "inselberg". However, equally, the coastal form may be of tectonic origin, because the western coast of the peninsula is controlled by a major NNW–SSE-striking, down-to-the-west normal fault interpreted from seismic profiles across the continental shelf of the Venezuela Gulf (Audemard, 1993).

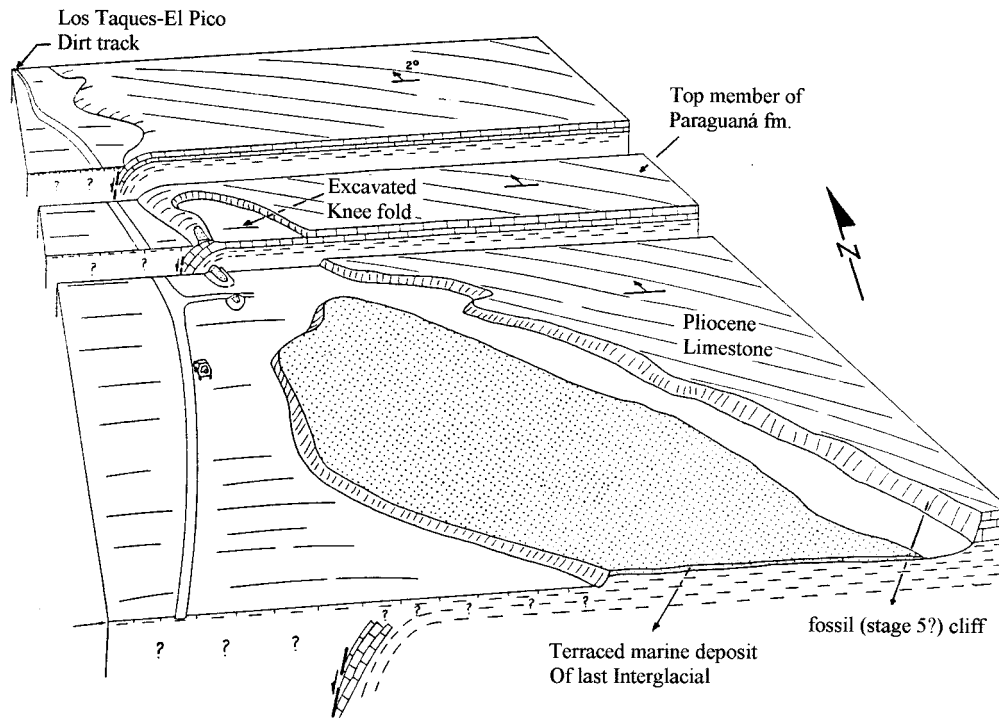The highest coastal cliffs coincide with the greatest nearshore bathymetric depths and also correspond to the

Fig. 17. Terraced marine deposit tentatively ascribed to isotope stage-5 highstand, located under a fossil marine cliff along the central segment of the western coast of the Paraguaná Peninsula (after Audemard, 1993). This unit post-dates folding, affecting the Pliocene Paraguaná Formation.

greatest vertical throw of the normal bounding fault (Fig. 10). If this reflects active tectonics, it is difficult to constrain the age of this activity, though it still appears to be controlling the present coastal configuration. Some Upper Pleistocene and Holocene marine features described by Audemard (1996b) would suggest that the peninsula is not being uplifted much because those features occur at heights predicted by global sea-level models and data. For example, a 6-km-long marine terrace, tentatively ascribed to isotope stage 5, occurs along the foot of the western coast fossil cliff, between Los Taques and Punta Salinas, at a maximum elevation of 5 m above sea level and therefore roughly in accordance with its expected elevation based on sea-level models. Similarly, a 4-m-high isolated remnant of the same marine located slightly south of Astinave, displays two notches on its seaward side: the lower one is the modern tidal notch, while the higher one probably corresponds to the +1-m-high Holocene sea-level highstand (4–2.5 Ka BP). Several other raised marine features along the eastern coast of mainland Falcón described by Audemard et al. (1997) appear to represent the same highstand. The implication of the coastal data is that the Paraguaná block has not been significantly uplifted during Holocene times, though the coastal evolution of this area still needs further detailed investigation.

Regardless of its Quaternary coastal history, the Paraguaná block must have uplifted sometime since the Pliocene because the marine facies of the Paraguaná Formation crop out at 80 above msl. Two plausible models, independent or combined, could explain this paradox. One model is that Paraguaná is not being currently uplifted but that instead the Venezuela Gulf shelf is sinking. This subsidence may imply active movement of the coast-bounding normal fault, but the absence of any compensatory shouldering effect (footwall uplift) onshore contrasts with the recognition of past uplift. This seems to fit perfectly with a normal fault where much dragging is taking place, as observed north of Los Taques (Fig. 17). An alternative model is that the vertical slip rate has diminished abruptly in Quaternary times. Support for the second model comes from the estimate by Audemard (1993), that the post-Pliocene slip rate of the Paraguaná Western Coast Fault is 0.08 mm/year, around half of the longer-term slip rate of 0.15 mm/year based on the vertical throw of the Middle Miocene unconformity, measured from subsurface data of the Venezuela Gulf shelf.

9. Discussion

The subtle, equivocal evidence for neotectonic activity on the Paraguaná Peninsula contrasts with the abundant evidence for recent both brittle and ductile deformations in the mainland, where microtectonic investigations are possible. However, in both areas, knowledge of the regional lithostratigraphic history is crucial to the success of subsequent microtectonic and neotectonic investigations.

Not all the tectonic structures described from the northern Falcón conform to the simple shear model proposed by
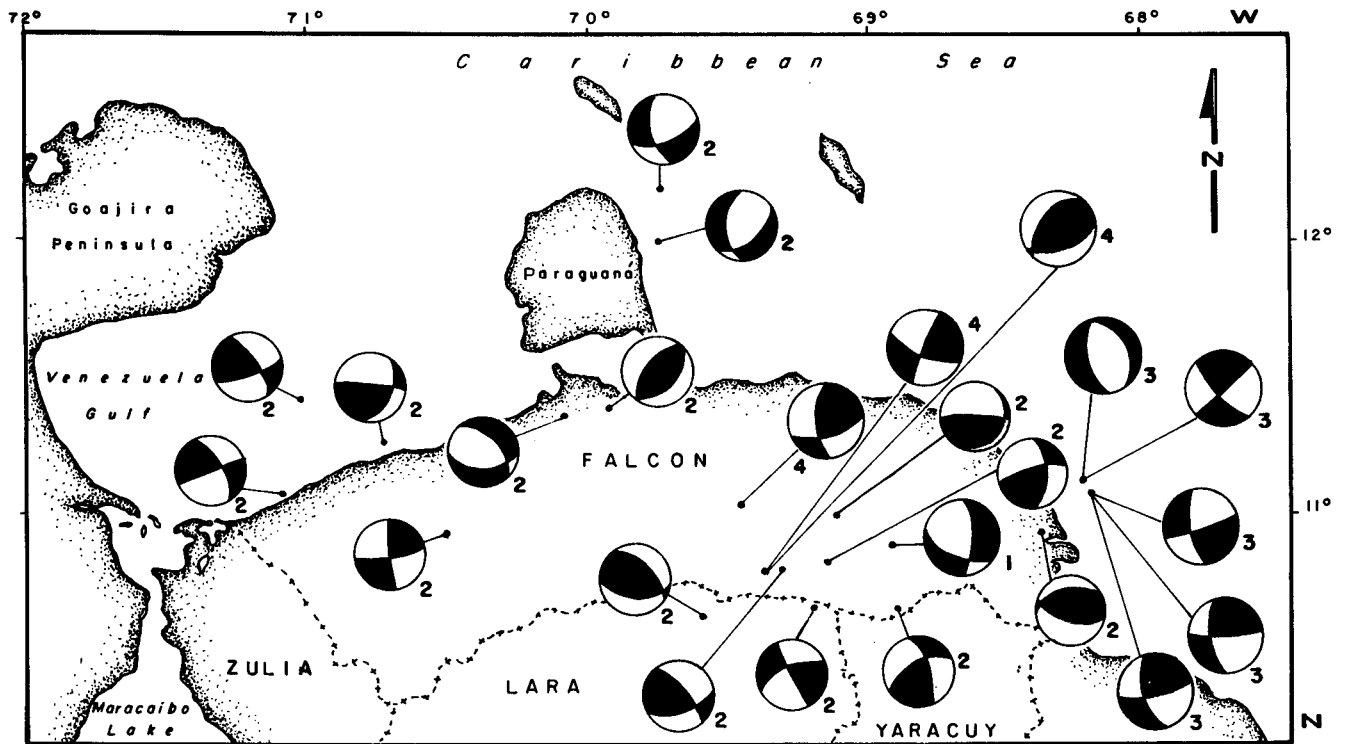
Fig. 18. Compilation of focal mechanisms solutions for the Falcón region (modified from Audemard, 1996b). Solutions labelled: (1) is from Dewey (1972; modified from Audemard and Romero, 1993); (2) were obtained from a microseismicity survey made in 1990 in an Intevep-CCE project (modified from Bach, 1991); (3) are from Malavé (1992); and (4) one from Audemard and Romero (1993).

Wilcox et al. (1973), but the structures do show coherence at regional scale. Furthermore, the neotectonic mapping and microtectonic investigations confirm the five families of faults outlined in the introduction. The stress tensor calculated from the general configuration of all these tectonic features is characterized by a NNW–SSE-trending σ_1 and ENE–WSW-trending σ_3, which represents a trans-current regime (intermediate stress in vertical position). This regime is consistent with the geodynamic setting of the northern Falcón Basin, especially given its proximity to the major east–west-trending right-lateral Oca-Ancón Fault separating the Bonaire and Maracaibo blocks. Locally, minor folding appears to coincide with restraining step-overs, such as between the two segments of the Urmaco Fault, and fault terminations, such as horse-tail splays at the northern tip of the Urumaco eastern segment. These are in good agreement with kinematics of the associated fault and with the derived stress tensor assuming the simple shear model.

Despite the small number of stress tensors calculated from microtectonic analyses of brittle deformation in the Pliocene and Quaternary sedimentary units of the northern Falcón, there is a good accordance between stress tensors derived from microtectonic data and that estimated previously from large-scale neotectonic structures. The results of the present study confirms that the region has undergone a compressive to compressive-transcurrent tectonic regime

during the Pleistocene, characterized by a NNW–SSE oriented maximum horizontal stress, and ENE–WSW-trending intermediate (or minimum) horizontal stress. However, with the exceptions of the Urumaco and Río Seco faults and the Guadalupe thrust, it is hard to extend this Quaternary activity into the Holocene. Nevertheless, the stress tensors derived from geologic data to focal mechanism solutions are consistent (compare Fig. 1 and Fig. 18), indicating that such tectonic regime still prevails in northern Venezuela. Thus, it can be argued that the boundary between the Bonaire and Maracaibo blocks traversing the Falcón Basin is transpressional and accommodates strain partitioning between wrenching along the right-lateral strike-slip Oca-Ancón fault system and subordinate trans-current faults and NNW–SSE-oriented shortening. The orientation of this stress tensor is persistent across the Carib-bean–South America realm, at least from Falcón on the west to Paria Peninsula on the east (Audemard et al., 1999b).

Against this regional geodynamic backdrop, the detailed microtectonic studies and the subsequent stress tensor deter-minations may shed light on important local deformation histories, for instance, block rotations between the two strands of the Río Seco Fault or progressive tectonic tilting of the Coro Formation stratotype deposit by the Guadalupe–Chuchure Thrust. However, some structures may not reflect the regional stress field and may instead respond to local

perturbations of the stress field, such as the folding at Punta Macolla (Audemard, 1993).

10. Conclusions

Inversion of the Falcón Basin started at about 17 Ma but it still seems active, based on the following observation: (1) the upright form of the Pliocene shallow marine deposits (La Vela Formation) along the northern limb of La Vela Anticline; (2) the northward tilt of the Plio-Pleistocene fanglomerates (Coro Formation); and (3) the existence of two young unconformities at the Miocene–Pliocene boundary and at sometime during the Lower Pleistocene.

Confirmation of the present persistence of this tectonic inversion is evident from the occurrence of both brittle and ductile deformations in Pliocene and Pleistocene formations that crop out in the northern Falcón Basin. Microtectonic data, based on some 400 measures of striations on either fault planes or cobble surfaces along with other kinematic indicators (e.g. gypsum fiber growth), analysed by the method of Etchecopar et al. (1981) has established that northern Falcón region is undergoing a regionally-consistent NNW–SSE to north–south maximum horizontal stress and an ENE–WSW-minimum (or intermediate) horizontal stress. The onset of this ongoing compressional phase certainly predates the progressive tilting of the Upper Pliocene–Lower Pleistocene fanglomerates of the Coro Formation and folding of the Pliocene Paraguaná Formation. In other words, the neotectonic activity is largely Quaternary (essentially Middle Pleistocene) in age, which is in agreement with the lithostratigraphic revaluation of this basin.

The calculated regional stress tensor is consistent with the stress field for the present-day kinematics of five families of active faults in this region. These families are: (1) east–west right-lateral faults; (2) NW–SE right-lateral faults, synthetic to the east-west faults; (3) NNW–SSE normal faults; (4) north–south to NNE–SSW left-lateral faults, antithetic to the east–west faults; and (5) ENE–WSW reverse faults, parallel to folding axis. The spatial configuration of these tectonic structures implies that the region is undergoing transpression analagous to the simple shear model proposed by Wilcox et al. (1973). This regional configuration results from right-lateral slip along the east–west trending Oca-Ancón Fault system, which separates the lithospheric blocks of Maracaibo and Bonaire. In turn, the NNE-directed extrusion of the Maracaibo and Bonaire blocks relates to the convergence between the Bonaire block and the Caribbean plate along the rather flat Southern Caribbean subduction located offshore the Netherland Antilles islands.

In terms of slip rate, most Quaternary tectonic features in Northern Falcón are slow, showing slip rates generally below 0.4 mm/year, with the exception of the major east–west striking right-lateral Oca-Ancón fault system whose rate is close to 2 mm/year.

References

Angelier, J., 1994. Fault slip analysis and paleostress reconstruction. In: Hancock, P. (Ed.), Continental Deformation. Pergamon Press, Oxford, pp. 53–100.

Audemard, F.A., 1993. Néotectonique, sismotectonique et aléa sismique du nord-ouest du Vénézuéla (système de failles d'Oca-Ancón). Ph.D. thesis, Université Montpellier II.

Audemard, F.A., 1996a. Field-trip guidebook to "The Upper Quaternary marine deposits of the Paraguaná Peninsula and Coro surroundings. 5th Annual CLIP Meeting, Cardón, Venezuela.

Audemard, F.A., 1996b. Upper Quaternary marine deposits of the Paraguana Peninsula, State of Falcon, northwestern Venezuela: preliminary geological observations and neotectonic implications. Quaternary International 31, 5–11.

Audemard, F.A., 1996c. Paleoseismicity studies on the Oca-Ancon fault system, northwestern Venezuela. Tectonophysics 259, 67–80.

Audemard, F.A., 1997. Tectónica activa de la región septentrional de la cuenca invertida de Falcón, Venezuela occidental. Proceedings, VIII Congreso Geológico Venezolano, Porlamar, pp. 93–100.

Audemard, F.A., 1998a. Bassin Tertiaire de Falcón, Vénézuéla nord-occidental: synthèse stratigraphique et inversion tectonique Mio-Quaternaire. Proceedings, XIV Caribbean Geological Conference, Trinidad, 1995, pp. 570–583.

Audemard, F.A., 1998b. Evolution géodynamique de la façade nord Sud-américaine: nouveaux apports de l'histoire géologique du Bassin de Falcón, Vénézuéla. Proceedings, XIV Caribbean Geological Conference, Trinidad, 1995, pp. 327–340.

Audemard, F.A., 1999. Morpho-structural expression of active thrust fault systems in the humid tropical foothills of Colombia and Venezuela. Zeitschrift für Geomorphologie 118, 1–18.

Audemard, F.A., Bousquet, J.-C., Rodríguez, J.A., 1999aa. Neotectonic and paleoseismicity studies on the Urumaco fault, northern Falcón basin, northwestern Venezuela. Tectonophysics 308, 23–35.

Audemard, F.A., Calassou, S., 1996. The Guadalupe-Mina de Coro-Chuchure Thrust fault system, Falcón Basin, Northwestern Venezuela: natural example and analog modelling of a transfer zone. Proceedings of Extended Abstracts, 3rd International Symposium on Andean Geodynamics, Saint-Malo, France, pp. 277–280.

Audemard, F.A., Rodríguez, J.A., Bousquet, J.-C., 1997. Holocene tectonic uplift of La Vela anticline related to the activity of the Guadalupe Thrust, northern Falcón State (Venezuela). Proceedings, IV CLIP Meeting, Canary Islands, 1995, pp. 13–27.

Audemard, F.A., Romero, G., 1993. The Churuguara area — Seismic evidence of contemporary activity of the Oca-Ancón system. Proceedings, Caribbean Conference on Natural Hazards: Volcanoes, Earthquakes, Windstorms, Floods. St. Augustine, Trinidad, pp. 21–32.

Audemard, F.A., Romero, G., Rendón, H., 1999b. Sismicidad, Neotectónica y Campo de Esfuerzos del Norte de Venezuela. Funvisis' unpublished report for PDVSA-CVP.

Audemard, F.A., Singer, A., 1996. Active fault recognition in northwestern Venezuela and its seismogenic characterization: neotectonic and paleoseismic approach. Geofísica Internacional 35, 245–255.

Audemard, F.A., Singer, A., Beltrán, C., Rodríguez, J.A., Lugo, M. Chacín, C., Adrianza, A., Mendoza, J., Ramos, C., 1992. Actividad tectónica cuaternaria y características sismogénicas de los sistemas de fallas de Oca-Ancón (Tramo Oriental), de la Península de Paraguaná y región de Coro y de la costa nororiental de Falcón. Funvisis' unpublished report for Intevep.

Audemard, F.A., De Mena, J., 1985. Falcón oriental, nueva interpretación estrución.

Baby, P., Spetch, M., Méndez, E., Guillier, B., Colletta, B., Letouzey, J., 1993. Development of transfer zones and location of oil and gas field in frontal part of Bolivian Andean fold-and-thrust belt. Proceedings of Abstracts, AAPG/SVG International Congress & Exhibition, Caracas, p. 36.

Bach, B., 1991. Interpretation und Analyse tektonischer Prozesse anhand mikroseismicher Messungen im Estado Falcon, Nordvenezuela. Master thesis, Universitat Hamburg.

Bell, J., 1972. Geotectonic evolution of the southern Caribbean area. Geological Society of America Memoir 132, 369–386.

Bellizzia, A., 1971. Mapa geológico Capatárida-Paraguaná-Puerto Cumarebo-Río Tocuyo-Río Matícora. M.M.H. Map N° 3. Scale 1:200,000.

Beltrán, C., 1993. Mapa Neotectónico de Venezuela. Funvisis. Scale 1:2,000,000.

Beltrán, C., Giraldo, C., 1989. Aspectos neotectónicos de la región nororiental de Venezuela. Proceedings, VII Congreso Geológico Venezolano, Barquisimeto, pp. 1000–1021.

Beltrán, C., Giraldo, C., 1989. Aspectos neotectónicos de la región nororiental de Venezuela. Proceedings, VII Congreso Geológico Venezolano, Barquisimeto, pp. 1000–1021.

Boesi, T., Goddard, D., 1991. A new geologic model related to the distribution of hydrocarbon source rocks in the Falcon Basin, northwestern Venezuela. In: Biddle, K. (Ed.), Active margins. American Association of Petroleum Geologists Memoir 48, pp. 303–319.

Bott, M., 1959. The mechanics of oblique slip faulting. Geol. Mag. 96, 109–117.

Cabrera de Molina, E., 1985. Evolución estructural de Falcón central. M.Sc. thesis, Universidad Central de Venezuela.

Calassou, S., Larroque, C., Malavieille, J., 1993. Transfer zones of defor-

mation in thrust wedges: an experimental study. Tectonophysics 221, 325–344.

Casagrande Fioretti, L., 1985. Evolution tectono-sédimentaire post-éocène de la bordure ouest du massif des Baronnies et du massif de Suzette (Chaines subalpines de Barronies). Ph.D. thesis, Université Paris XI.

Combes, P., 1984. La tectonique récente de la provence occidentale: micro-tectonique, caractéristiques dynamiques et cinématiques. Méthodologie de zonation tectonique et relations avec la sismicité. Ph.D. thesis, Université de Strasbourg.

Cross, R., 1952. Geology of North Central Falcón. Maraven, S.A.'s EPC10.111 unpublished company report.

Danielo, A., 1976. Formes et dépôts littoraux de la côte septentrionale du Vénézuéla. Annales de Geographie 85, 68–97.

Dewey, J., 1972. Seismicity and tectonics of western Venezuela. Bulletin of the Seismological Society of America 62 (6), 1711–1751.

Etchecopar, A., Vasseur, G., Daignieres, M., 1981. An inverse problem in microtectonics for the determination of stress tensors from fault striation analysis. Journal of Structural Geology 3, 51–65.

Feo-Codecido, G., 1971. Guía de la excursión a la Península de Paraguaná, Estado Falcón. Boletín Geológico. Publicación Especial 5, 304–315.

Ferrell, A., Romero, P., Rodríguez, C., 1969. Geology of the West Falcón sub-basin, Venezuela texpet. Maraven, S.A.'s EPC-5792 unpublished company report.

Freymueller, J.T., Kellogg, J.N., Vega, V., 1993. Plate motions in the north Andean region. Journal of Geophysical Research 98, 21853–21863.

González de Juana, C., 1937. Geología general y estratigrafía de la región de Cumarebo, estado Falcón. Boletín de Geología y Minería (Venezuela) 1, 195–218.

González de Juana, C., 1972. Guía de la excursión a la estructura de La Vela de Coro (Falcón). Proceedings, IV Congreso Geológico Venezolano. Boletín de Geología, Publicación Especial 5, pp. 317–327.

Graf, C., 1969. Estratigrafía cuaternaria del noroeste de Venezuela. Boletín Informativo, Asociación Venezolana de Geología. Minería y Petróleo 12, 393–416.

Hancock, P., Barka, A., 1987. Kinematic indicators on active normal faults in western Turkey. Journal of Structural Geology 9, 573–584.

Jaeckli, R., Erdman, D., 1952. Geological compilation report: Central and West Falcón. Maraven S.A's EPC-1272 unpublished company report.

Jordan, T., 1975. The present-day motion of the Caribbean plate. Journal of Geophysical Research 80, 4433–4439.

Kavanagh de Petzall, C., 1959. Estudio de una sección de la Formación Caujarao en el anticlinal de La Vela, Estado Falcón. Boletín Informativo, Asociación Venezolana de Geología. Minería y Petróleo 2, 269–318.

Malavé, G., 1992. Inversión de ondas de volumen de algunos sismos importantes del noroccidente de Venezuela: relación con la tectónica regional. Master thesis, Instituto de Geofísica, UNAM, México.

Malfait, B., Dinkelman, M., 1972. Circum-Caribbean tectonic and igneous activity and the evolution of the Caribbean plate. Bulletin of the Geological Society of America 83, 251–272.

Mattauer, M., 1973. Les déformations des matériaux de l'ecorce terrestre. Hermann, Paris.

Méndez, J., Guevara, E., 1969. Geological compilation map of N.W. Venezuela, Guajira and Aruba. Shell map, scale 1:250,000.

Minster, J., Jordan, T., 1978. Present-day plate motions. Journal of Geophysical Research 83, 5331–5354.

Molnar, P., Sykes, L., 1969. Tectonics of the Caribbean and Middle America regions from focal mechanisms and seismicity. Bulletin of the Geological Society of America 80, 1639–1684.

Pérez, O., Aggarwal, Y., 1981. Present-day tectonics of southeastern Caribbean and northeastern Venezuela. Journal of Geophysical Research 86, 10791–10805.

Petit, J.-P., Proust, F., Tapponnier, P., 1983. Critères de sens de mouvement sur les miroirs de failles en roches non calcaires. Bulletin Societé géologique de France XXV, 589–608.

Pindell, J., Dewey, J., 1982. Permo-Triassic reconstruction of western Pangea and the evolution of the Gulf of Mexico/Caribbean region. Tectonics 1, 179–211.

Proust, F., Petit, J-P., Tapponnier, P., 1977. L'accident du Tizi n'Test et le rôle des décrochements dans la tectonique du Haut Atlas occidental (Maroc). Bulletin Societé géologique de France XIX, 541–551.

Ritz, J.-F., 1991. Évolution du champ de contraintes dans Les Alpes du sud depuis la fin de l'Oligocène. Implications sismotectoniques. Ph.D. thesis, Université de Montpellier II.

Rod, E., 1956. Strike-slip faults of northern Venezuela. Bulletin American Association of Petroleum Geologists 40, 457–476.

Schrader, F., 1988. Symmetric of pebble-deformation involving solution pits and slip-lineations in the northern Alpine Molasse Basin. Journal of Structural Geology 10, 41–52.

Schubert, C., 1984. Basin formation along Boconó-Morón-El Pilar fault system, Venezuela. Journal of Geophysical Research 89, 5711–5718.

Singer, A., Audemard, F.A., 1997. Aportes de Funvisis al desarrollo de la geología de fallas activas y de la paleosismología para los estudios de amenaza y riesgo sísmico. In: Grases, J (Ed.), Diseño sismorresistente: especificaciones y criterios empleados en Venezuela. Publicación Especial de la Academia de Ciencias Físicas, Matemáticas y Naturales, 33, pp. 25–38.

Slemmons, D., 1977. Faults and earthquake magnitudes. Miscellaneous paper S-73-1, U.S. Army Engineer Waterways Experiment Station, Vicksburg.

Soulas, J.-P., 1986. Neotectónica y tectónica activa en Venezuela y regiones vecinas. Proceedings, VI Congreso Geológico Venezolano, Caracas, 1985, pp. 6639–6656.

Soulas, J.P., Giraldo, C., Bonnot, D., Lugo, M., 1987). Actividad cuaternaria y características sismogénicas del sistema de fallas Oca-Ancón y de las fallas de Lagarto, Urumaco, Río Seco y Pedregal. Afinamiento de las características sismogénicas de las fallas de Mene Grande y Valera. (Proyecto COLM). Funvisis' unpublished company report for Intevep.

Stephan, J.-F., 1982. Evolution géodinamique du domaine Caraïbe, Andes et chaîne Caraïbe sur la transversale de Barquisimeto (Vénézuéla). Ph.D. thesis, Université de Paris VI.

Stephan, J.-F., 1985. Andes et chaîne Caraïbe sur la transversale de Barquisimeto (Vénézuéla): évolution géodinamique. Proceedings, Symposium Géodynamique des Caraïbes, Paris, pp. 505–529.

Sykes, L., McCann, W., Kafka, A., 1982. Motion of Caribbean Plate during last 7 million years and implications for earlier Cenozoic movements. Journal of Geophysical Research 87, 10656–10676.

Taboada, A., 1993. Stress and strain from striated pebbles. Theoretical analysis of striations on a rigid spherical body linked to a symmetrical tensor. Journal of Structural Geology 15, 1315–1330.

Tjia, H., 1971. Fault movement reoriented stress field and subsidiary structures. Pacific Geology 5, 49–70.

Vallenilla, P., 1953. Estratigrafía de las formaciones Caujarao, La Vela y Coro en sus localidades tipos, Estado Falcón. Undegraduate thesis, Universidad Central de Venezuela.

Vallenilla, P., 1961. Estratigrafía de las formaciones Caujarao, La Vela y Coro en sus localidades tipos, Estado Falcón. Boletín Informativo. Asociación Venezolana de Geología, Minería y Petróleo 4, 29–78.

Vedder, J., Wallace, R., 1970. Map showing recently active breaks along the San Andreas and related faults between Cholame Valley and Tejon Pass, California: U.S. Geological Survey Miscellaneous Geologic Investigations Map I-574. Scale 1:24,000.

Wadge, G., Burke, K., 1983. Neogene Caribbean plate rotation and associated central American tectonic evolution. Tectonics 2, 633–643.

Wesson R., Helley, E., Lajoie, K. Wentworth, C., 1975. Faults and future earthquakes U.S. Geological Survey Professional Paper P941A.

Wiedenmayer, C., 1937. Informe geológico sobre los depósitos carboniferos de Coro, Distrito Miranda, Estado Falcón. Boletín de Geología y Minería (Venezuela) 1, 1–65.

Wilcox, R., Harding, T., Seely, D., 1973. Basic wrench tectonics. Bulletin of the American Association of Petroleum Geologists 57, 74–96.

Wozniak, J., Wozniak, M., 1979. Geología de la región de Cabure Estado Falcón. M.E.M.'s unpublished report.

Zeigler, J., 1964. The hydrography and sediments of the Gulf of Venezuela. Limnology and Oceanography 9, 397–411.